NASA CR-174666
PWA-5833-37

NASA

ABRASIVE TIP TREATMENT FOR USE ON COMPRESSOR BLADES

H. C. Pedersen

UNITED TECHNOLOGIES CORPORATION
Pratt & Whitney Engineering Division
East Hartford, Connecticut 06108

Prepared for

NATIONAL AERONAUTICS AND SPACE ADMINISTRATION

Lewis Research Center
Cleveland, Ohio 44135

Contract NAS3-22813

1. Report No. NASA CR-174666	2. Government Accession No.	3.Recipient's Catalog No.
4. Title and Subtitle Abrasive Tip Treatment for Use on Compressor Blades		5. Report Date January, 1984 6. Performing Organization Code
7. Author(s) Herbert C. Pedersen		8. Performing Org. Rept. No. PWA-5833-37
9. Performing Organization Name and Address UNITED TECHNOLOGIES CORPORATION Pratt & Whitney Engineering Division East Hartford, Connecticut 06108		10. Work Unit No. 11. Contract or Grant No. NAS3-22813
12. Sporsoring Agency Name and Address NATIONAL AERONAUTICS AND SPACE ADMINISTRATION Lewis Research Center/ U.S. Army Research and Technology Laboratories (AVSCOM) Propulsion Laboratory 21000 Brookpark Road; Cleveland, Ohio 44135		13. Type Rept./Period Covered Contractor Report 14. Sponsoring Agency Code 1L161102AH45

15. Supplementary Notes
Project Manager; Robert F. Handschuh
U.S. Army Research and Technology Laboratories (AVSCOM), Propulsion Laboratory
NASA Lewis Research Center; Cleveland, Ohio 44135

16. Abstract

During this program, five plasma sprayed matrices and three abrasive grit materials were evaluated for use as an abrasive tip treatment for use on compressor blades. The plasma spray deposition of the abrasive tip treatment was accomplished using a "co-spray" process. This process simultaneously but separately introduces the abrasive grits and metal matrix powder into the plasma stream and entraps the abrasive grits within a molten matrix to form an abrasive coating as the matrix material solidifies on the test specimen surfaces. Spray trials were conducted to optimize spray parameter settings for the various matrix/grit combinations before actual spraying of the test specimens.
Rub, erosion, and bond adhesion tests were conducted on the coated specimens in the as-sprayed condition as well as on coated specimens that were aged for 100 hours at a temperature of 866K (1100°F). Microscopic examinations were performed to determine the coating abrasive-particle content, the size and shape of the adhesive particles in the coating, and the extent of compositional or morphological changes resuting from the aging process.
After testing, the data were reduced and evaluated to determine the best matrix/abrasive combination for use as an abrasive tip treatment on compressor blades. A nickel chromium/aluminum composite with No. 150 size (0.002 to 0.005 inch) silicon carbide grits was selected as the best matrix/abrasive combination of the candidates surveyed.

17. Key Words [Suggested by Author(s)]	18. Distribution Statement
Gas Path Sealing Blade Tip Clearance Blade Tip/Shroud Rub Plasma-Sprayed Abrasive Compressor Efficiency Abrasive Grits	

19. Security Class (This Rept)	20. Security Class (This Page)	21. No. Pgs	22. Price *
UNCLASSIFIED	UNCLASSIFIED		

* For sale by the National Technical Information Service, Springfield, VA 22161

FOREWORD

This report describes the work accomplished under Contract NAS3-22813, Abrasive Tip Treatment for Use on Compressor Blades, by Pratt & Whitney (P&W) Engineering Division, United Technologies Corporation for the Lewis Research Center of the National Aeronautics and Space Administration. The technical effort was initiated on May 21, 1981 and completed on September 21, 1983.

Mr. Robert C. Bill of the National Aeronautics and Space Administration (NASA) was the initial Project Manager and Mr. David M. Thomas was the initial Contracting Officer. During the course of the contract, Mr. Robert F. Handschuh was assigned as Project Manager, and Mr. Anthony Long was assigned as Contracting Officer.

This report was prepared by Mr. Herbert C. Pedersen, the Program Manager for Pratt & Whitney.

The plasma spray coating, metallographic analysis, and tensile test work required for the contract was conducted by the United Technologies Research Center (UTRC) of United Technologies Corporation. Appreciation is gratefully acknowledged to the following UTRC and P&W personnel for their assistance: Richard C. Novak, Senior Materials Scientist, and Dr. Harry E. Eaton, Materials Research Engineer, both of UTRC, who developed the plasma "co-spray" process used in this contract, for providing the plasma-spray, adhesion test, and metallographic services and analysis; Thaddeus J. Zebrowski, P&W Analytical Engineer for his assistance in conducting the test program and data analysis; and James L. Migliore, P&W Engineering Technician, for conducting the rub tests and related data reduction.

TABLE OF CONTENTS

LIST OF ILLUSTRATIONS

LIST OF ILLUSTRATIONS (Continued)

LIST OF ILLUSTRATIONS (Continued)

SECTION 1.0

SUMMARY

This program was conducted to test and evaluate candidate plasma-sprayed materials for use as an abrasive tip treatment on compressor blades. This section describes the testing program, summarizes the results of those tests, and presents a statement of the conclusions that were drawn on the basis of the test results.

Five metal matrix materials (METCO 16C, METCO 443, METCO 43C, TRIBALOY, and TIPALOY) in selective combination with three abrasive grits (silicon carbide, aluminum oxide, and silicon nitride) were evaluated for use as a plasma sprayed abrasive tip treatment on compressor blades. The effects on coating integrity of grit size, grit concentration, and aging for 100 hours at 866K (1100°F) were also evaluated. The results of data obtained from rub, erosion, and adhesion tests in conjunction with microscopic examinations of the coating composition formed the basis for this evaluation.

In order to obtain the desired grit concentration levels with minimum porosity (voids) in the abrasive coating, plasma spray trials of small 0.76-mm (0.030-inch) thick simulated blade tip cross sections were conducted, followed by microscopic examinations. Large scale porosity was of concern since voids reduce bonding between the grits and the matrix binder, thereby reducing the coating strength. Porosity could not be eliminated entirely, and it was found that the level of porosity inherently increased during the spray process as coating grit size or grit concentration levels were increased.

Abrasive grits larger than No. 150 size (0.002-0.005 inch) are very difficult to spray on thin 0.76mm thick blade tips. The self erosive nature of the large grits results in a random capturing of the grits in the matrix during the spray process, thus making grit concentration and distribution almost impossible to control with any degree of confidence. The maximum grit concentration attainable with acceptable porosity was approximately 20 to 30 percent with small No. 150 grit sizes and 10 to 15 percent for grit sizes larger than No. 90 (0.005-0.008 inch).

Microscopic examination of the candidate coating materials plasma sprayed onto titanium, nickel, and iron-based alloy substrates exhibited no evidence of chemical reactions between the coatings and substrates. Some chemical reaction, however, was observed between METCO 16C matrices and silicon carbide grits during the aging process. Significant microcracking was evident in coatings comprised of Tribaloy 400 and METCO 16C matrices. Aging improved the abrasive performance and erosion resistance of most coatings sprayed with small abrasive grits.

The abrasive performance of the candidate coating materials was determined by conducting comparative rub tests and converting the results to volume wear ratio (volume of abradable seal material removed per volume of blade wear)

which is a measure of the abradability of a seal system. The results clearly show that abrasive coatings on the blade tips results in improved abradability. For a given coating composition, small grits with low 20 to 30 volume percent grit concentration levels exhibit better abrasive performance than large grits at similar concentration levels. Tangential and normal rub force measurements were attempted during these tests using a piezoelectric force measurement instrumentation system. These measurements, however, could not be interpreted properly due to the masking of the force signals by extraneous signals, generated by resonant vibrations inherent to the rig mounting system that could not be "tuned" out.

The erosion resistance of the candidate coating materials evaluated in a high-velocity erosion rig at room temperature is considerably lower (50 to 200 percent) than that determined for uncoated titanium, nickel, and iron-based alloy materials typically used for compressor blades. Erosion is material dependent, resulting in noticeable erosion resistance differences between the candidate coating materials. Grit material or concentration level, however, did not appear to significantly effect erosion resistance.

Coating bond strength, based on the average of three adhesion tests, varied from 1378 N per cm^2 (2000 pounds per $inch^2$) to greater than 6895 N per cm^2 (10,000 psi), depending on the candidate material tested; in general, the bond strength improved with aging.

Conclusions based on the results of the test program described above are summarized below:

- Of the candidates surveyed, METCO 443 (nickel chromium/aluminum composite) in combination with No. 150 silicon carbide abrasive grits, at a 20 to 30 percent volumetric grit concentration level, is the best matrix/abrasive coating material combination.

- The use of abrasive grits larger than No. 150 in size are not recommended because they:

  - are difficult to plasma spray onto thin compressor blade tip cross sections;
  - do not improve the rub performance and erosion resistance qualities of the coating; and
  - tend to reduce the coating bond strength.

- Aging of the coatings at a temperature of 866°K (1100°F) for 100 hours improves their abrasive and erosion resistance qualities.

- Coating porosity increases with increased grit concentration and grit size.

SECTION 2.0

INTRODUCTION

Gas path sealing is a critical factor in gas turbine engine performance and fuel consumption. As the engine cycle has moved toward higher compressor pressure ratios, blade tip clearance in the high-pressure compressor has become a subject of increasing concern. If the detrimental effects of tip leakage are to be minimized, engines must be able to operate with minimum tip clearance at all flight conditions while avoiding interference between blade tip and shroud through all engine transients. Additionally, the engine must be designed to successfully withstand bladetip/shroud rubs resulting from maneuver and surge deflections. Since the clearance increase produced by rubbing wear will be minimized if the wear occurs preferentially on the shroud with negligible wear on the blade tips, static shrouds in modern gas turbine engines incorporate surface layers of abradable materials.

Compressors operating with minimum blade tip clearances undergo periodic rub interactions which, with current technology seal systems in some applications, lead to increased operating clearances as a result of blade tip wear. In addition, rub-induced damage can seriously affect engine integrity and, because of the extensive use of titanium-based alloys in compressors, can lead to titanium ignition. Coating of the blade tips with an abrasive will serve to both reduce blade wear and increase seal abradability.

Metal-cutting microstructures generate far less rub energy for removal of a given volume of seal material than do wear resistant coatings. Thus, abrasive blade tip treatment would extend the range of rub conditions that the blade-tip/seal system could tolerate without increasing rub tip wear. The development of technology for the plasma-spraying of an abrasive tip treatment onto compressor blades would minimize operating clearances between rotating blade tips and the stationary casing, thus increasing compressor efficiency by reducing leakage.

2.1 BACKGROUND

The purpose of compressor tip seals is to minimize the leakage air across the blade tips from the pressure to the suction side of the blades. Such leakage results in irrecoverable losses which translate into compressor efficiency loss. Since an aerodynamically smooth surface is needed for the compressor end wall, tip sealing is accomplished by maintaining a minimum clearance between the blade tip and the opposing shroud. Beyond the tolerance limitations inherent in various fabrication and assembly procedures, there are a number of factors which lead to compressor tip clearance variations during engine operation. These are maneuver and landing g-loads, rotor and stator deflection during off-design engine operation (for example, surge-induced deflection), thermal transient mismatch between rotating and static seal components, rotor whirl, engine case distortion due to engine mount loads, and structural vibration and instability. For engines which are built with initially tight tip clearances, these effects result in rubbing between the blade tips and shroud which produces wear of the blades or the shroud, or

both, with an attendant increase in tip clearance. Shrouds that are truly abradable result in localized shroud wear, rather than full circumferential blade wear, and thus result in a minimun increase in tip leakage due to rub interactions. The abradables used in current engines only partially meets this objective. The resulting blade wear has not only produced immediate losses in engine performance but has become a major cost factor in engine overhaul since worn blades must be replaced in order to restore a compressor to its original efficiency and flow capacity.

The primary objective for an abradable material is that it be readily removable by the rubbing action of the compressor blades. Since it is advantageous for blade tip thickness to be minimized for aerodynamic performance and for the blade material to be dictated by overall structural requirements, acceptable abradability requires achievement of a low density, preferably friable seal material. Unfortunately, this objective is in opposition to the other two major design considerations, erosion resistance and high temperature stability. The material choice for all abradable systems must provide an effective trade between durability and abradability, taking into account the engine rub history and operating environment (temperature, pressure, flow field, erosion climate, and the time factor). Other factors which must be considered in the design of abradable blade tip seal systems include minimum cost, field refurbishment capability, a rotor/stator thermal response match, and minimum weight.

Another method to improve the effectiveness of abradable seal systems is to treat the blade tips with an abrasive coating that will cut away the abradable material with minimum wear of the blade tip coating. These coatings should provide good abrasive qualities and yet provide asperities sufficient to remove rub debris without plugging. Abrasive grits entrapped in a metallic matrix ("glue") and applied as a coating to the blade tips by a plasma spray process would provide these qualities. The work conducted under this program concentrated on the development of a plasma spray process to apply the coating and the test evaluation of candidate abrasive and matrix materials to select a viable system for the abrasive treatment of compressor blade tips.

2.2 PROGRAM OVERVIEW

The objective of this program was to develop a plasma-sprayed coating for compressor blade tips that operates on the principle of metal cutting rather than wear resistance. The advantage of this approach is that metal cutting microstructures produce far less rub energy for removal of a given volume of seal material than do wear resistant coatings. The general approach that was followed was to separately introduce the tip coating binder material and the fine abrasive particulates into the plasma-spray stream so that the sharp cutting geometry of the abrasive particles is preserved in the as-sprayed coating. To accomplish this objective, five matrix materials and three abrasive powders were selected, sprayed on specimens, microscopically examined for coating defects, and tested for bond adherence, erosion resistance, and abrasive rub characteristics. Since proper selection of these materials required consultation with personnel with expertise in the fields of metallurgy, plasma spraying, and materials, a committee staffed with seven experts was formed to make this initial selection.

Since plasma spraying is sensitive to many parameters, such as gun distance, electrical power, spray velocity, powder flow, etc., initial spraying trials were conducted to define these parameters prior to the actual spray coating of the specimens for test and evaluation.

Initially, combinations of two abrasive grit materials (SiC and Al_2O_3), of No. 150 grit size and four matrix powders (METCO 16C, METCO 43C, METCO 443, and TRIBALOY T-400) were spray coated onto titanium alloy specimens using two target abrasive grit concentration levels (25 and 50 percent by volume) for testing. Test evaluations were conducted on each matrix/abrasive coating combination in the as-sprayed condition and after aging in air for 100 hours at 866K to assess the coating rub characteristics, erosion resistance, and bond adherence. Microscopic examinations were performed to detect any metallurgical degradation that had occurred due to the spray process or aging. The results of these data were evaluated and graded to determine the best single treatment and abrasive concentration for further evaluation.

The best coating system, selected from these initial screening tests, was sprayed onto typical compressor-blade material (titanium, nickel, and iron based alloy) specimens and test evaluated. In addition, the effects of larger No. 90 and No. 54 grit sizes on coating integrity as well as a higher temperature capability tipaloy matrix and Si_3N_4 abrasive grit material were test evaluated for use as an abrasive tip treatment on compressor blades.

Page Intentionally Left Blank

SECTION 3.0

TECHNICAL DISCUSSION

3.1 SELECTION OF MATERIALS

Cutting ability is the prime consideration in the selection of materials for development of the abrasive tip treatment coating. The compressor blade tip treatment must provide a sharp cutting surface, formed by abrasive grits, that will machine away the shroud during rub interactions without material transfer which can cause plugging of the cutting surface. The abrasive cutting ability depends on both strength and shape of the grit. Hard, sharp, faceted grits are capable of cutting rather than plowing the seal surface, and proper spacing of the grit will minimize build-up of the wear debris and bridging of the grits, thereby maintaining cutting efficiency. The requirement for selection of grits is, therefore, that the grits be hard and sharp and maintain these characteristics during the fabrication process and in the engine environment, particularly during a rub.

The matrix material must provide a durable bond of the grit material to the blade and must, therefore, be compatible with both the blade and grit materials. Temperature capability, strength, and oxidation resistance are all necessary characteristics.

Because the selection of materials for a plasma-sprayed abrasive coating involves many considerations from various related disciplines, a committee of seven technical specialists, with expertise in the fields of plasma-spray application, metallography, materials, seal systems development, and rub dynamics, was formed to make these selections. In the selection of the candidate matrix powder and abrasive grit powder compositions for use in the compressor blade composite coating experiments, a number of important variables were considered; these variables are:

- Chemical compatibility between the matrix, substrate, and abrasive grits;
- Physical properties including thermal expansion characteristics and strength at operating temperature;
- Oxidation and corrosion resistance;
- Availability; and
- Ease of application.

Based on consideration of the above variables, the committee selected the following matrix powders and abrasive grit powders for use in the abrasive coating experimental evaluations.

3.1.1 Matrix Powders

METCO 16C - A self-fluxing nickel-chromium powder of 16% chromium, 4% silicon, 4% boron, 3% copper, 3% molybdenum, 2.5% iron, 0.5% carbon, and the balance, nickel; powder size range, -120 to +325 mesh.

METCO 43C-NS - An 80% nickel, 20% chromium alloy powder which is more ductile than METCO 443-NS; powder size range, -140 to +325 mesh.

METCO 443-NS - A nickel-chromium/aluminum, composite powder of 6% aluminum and the balance, a nickel-chromium alloy, The nickel reacts exothermally with the aluminum during plasma spraying to produce a high bond strength coating. This material is commonly used as a bond coat for other plasma-sprayed material coatings; powder size range, -120 to +325 mesh.

TRIBALOY 400 - A 62% cobalt, 28% molybdenum, 2% silicon, and 8% chromium alloy powder which structurally has a hard intermetallic phase dispersed in a softer matrix of eutectic or solid solution. The intermetallic phase is a Laves phase type of cobalt, molybdenum, and silicon. This material produces a hard, wear resistant coating with good bond strength; powder size, -325 mesh.

TIPALOY - A 56% nickel base alloy with 25% chromium, 8% tungsten, 4% tantalum, 6% aluminum, 1% hafnium, 0.1% yttrium, and 0.23% carbon. It has good oxidation resistance and high creep strength at temperatures in excess of 1367K (2000°F); powder size range, -270 to +325 mesh.

The above matrix powders that were selected for evaluation all have good to excellent corrosion and oxidation resistance, have good bond strength, and can be used at temperatures up to 1255K (1800°F); Tipaloy has a useful temperature in excess of 1367K (2000°F).

3.1.2 Abrasive Grit Powders

Silicon carbide - Grits with numerous, hard sharp-edged facets that provide good cutting capability, have a useful temperature range of more than 1920K (3000°F), and have good wear resistance. These grits tend to react with nickel and other metals at temperatures above 1030K (1400°F).

Aluminum oxide - Grits that are very stable, do not react with other metals, and have a useful temperature range of more than 1920K (3000°F). These grits have numerous sharp-edged facets but do not have the wear resistance of silicon carbide grits when exposed to rub situations.

Silicon nitride - Grits that are hard and stable, do not react with other metals, and have a useful range of more than 1920K (3000°F). They have a wear resistance that is better than that of aluminum oxide but not as good as that of silicon carbide.

To minimize cost, the grit size ranges selected were primarily based on commercial availability. Silicon nitride was the one exception; it was purchased in block form, crushed, and screened to size in the laboratory.

3.2 PREPARATION OF SPECIMENS

Various methods of fabricating abrasive tips for blades offer potential and have been developed. Hot Isostatic Pressing and electroplating are the most common current means for depositing abrasive grits on turbine blades. These fabrication processes are relatively complex and expensive. The plasma spray process is by far the potentially least costly method of fabrication.

The plasma spray deposition of the abrasive tip treatment was accomplished using a "co-spray" process. In this process, a plasma gas stream is generated in a plasma gun, and metal matrix particles are injected into the hot plasma stream immediately downstream of the plasma nozzle; the abrasive grit particles are injected into the plasma stream at a point nearer to the surface to be coated than the point of injection of the metal matrix particles.

To provide the separate matrix powder and abrasive powder injection ports required for "co-spraying", a standard METCO 7M spray gun was modified to incorporate a secondary port for grit injection. This secondary grit injector is a 6.3 mm (0.25-inch) diameter tube attached to the spray gun and is oriented to inject the grit particles perpendicular to the spray axis, see Figure 1. The grit injector is located downstream and is aimed to be opposing the matrix injector. This position, in conjunction with other plasma-spray system parameters, must be optimized for each matrix/abrasive grit powder combination.

The abrasive coating is achieved by the entrapment of the grit particles in the molten metal matrix material as the matrix material solidifies and deposits on the surface to be coated. The purpose of "co-spraying" rather than spraying a blend of grit and matrix is to allow the independent optimization of the heat treatment of the two component materials. This process preserves the original sharp angular surfaces of the grit since it can be captured in the matrix without melting. To distribute the abrasive mixture evenly along the surface of the test specimens, the specimens were mounted in a fixture that rotates them through the plasma spray effluent.

"Co-spraying" of an abrasive coating requires special skills and techniques to achieve the desired results. Many spray parameters, such as electric power, arc gas flow, matrix and abrasive powder flow, gun distance, spray time, etc., must be optimized before the actual test specimens are coated. By conducting trial sprays, sectioning the coatings, and performing microscopic examinations the spray parameters required to produce the desired coatings for experimental evaluation were obtained.

Based on past experience in developing the "co-spray" process, systematic trial sprays were conducted to define the many parameters required for plasma spraying the various tip treatment combinations for this program. The sensitivity of grit concentration to the major spray parameters, based on this past work, is illustrated in Figure 2. These parameters must be optimized for each: 1) matrix/abrasive grit material combination, 2) grit concentration level, 3) grit size, and 4) substrate material being coated.

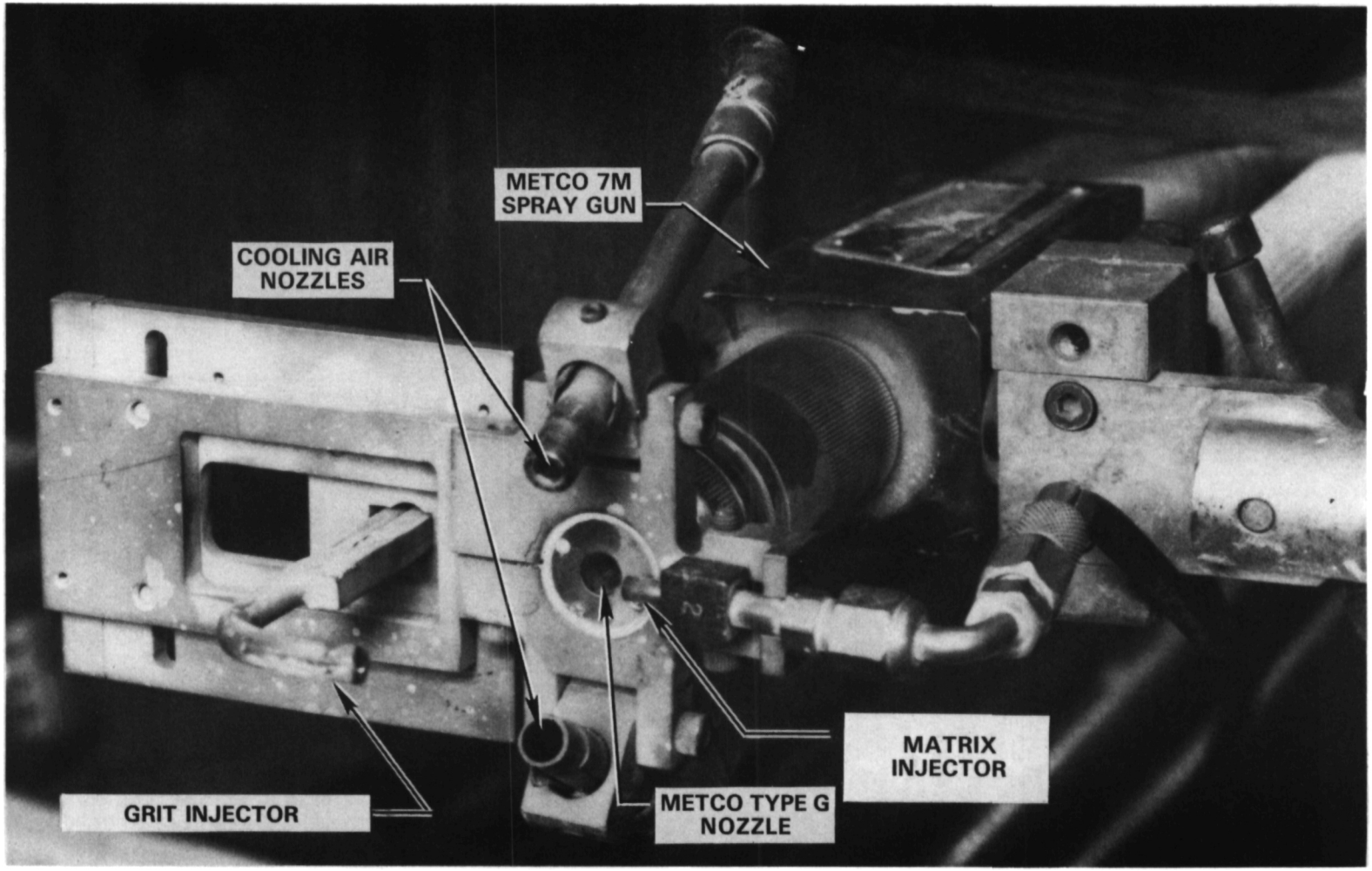

Figure 1 METCO 7M Spray Gun Equipped for Plasma Spraying.

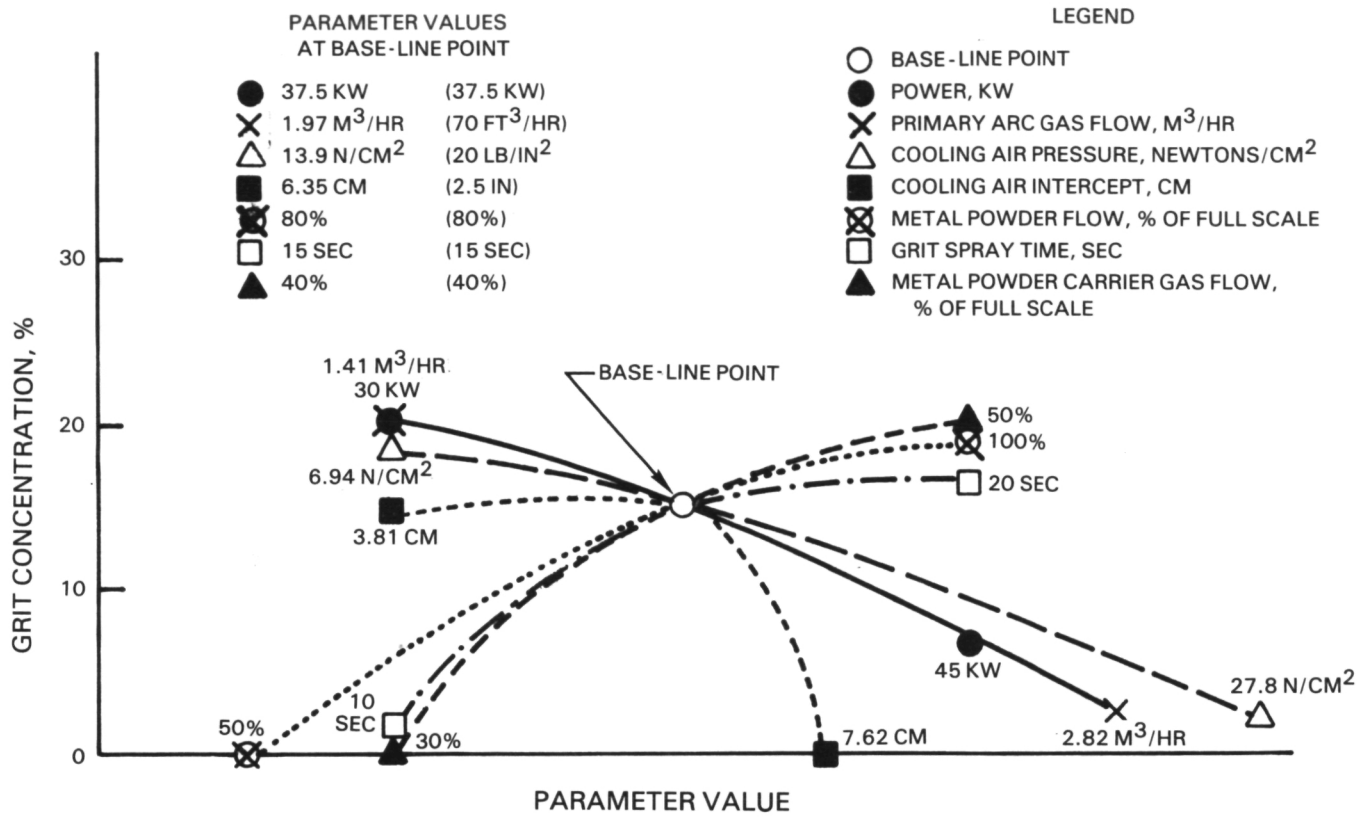

Figure 2 Grit Concentration Sensitivity to Spray Parameters.

The trial sprays were conducted on sheet metal substrates of the same material and tip dimensions as the simulated blades used for the rub test portion of this program. This was done to ensure that geometry and material effects would not mask the interpretation of microscopic examinations performed to assess the coating quality and grit concentration level.

Based on extensive spray trials, three key parameters (grit injector-to-substrate distance, primary plasma arc gas flow, and amperage) were identified as requiring major optimization for controlling coating grit concentration levels for each tip treatment system. Grit injector-to-substrate distance, however, requires optimization only for grit size variation. Figure 3 shows that decreasing the grit injector-to-substrate distance increases grit concentration, however, with a related increase in coating porosity. Porosity increases with grit concentration due to the shadowing of the close packed grits which prevents good filling of the matrix material around the grits. Reducing primary arc gas flow results in increased grit concentration and is illustrated in Figure 4; again, increased porosity is exhibited with increased grit concentration. As can be seen in Figure 5, increasing plasma gun amperage has the effect of reducing grit concentration level.

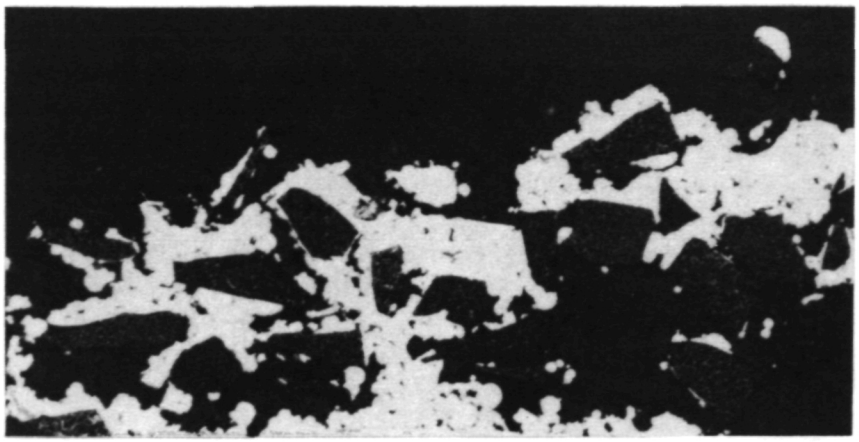

GRIT INJECTOR DISTANCE = 1.59 MM (100X)

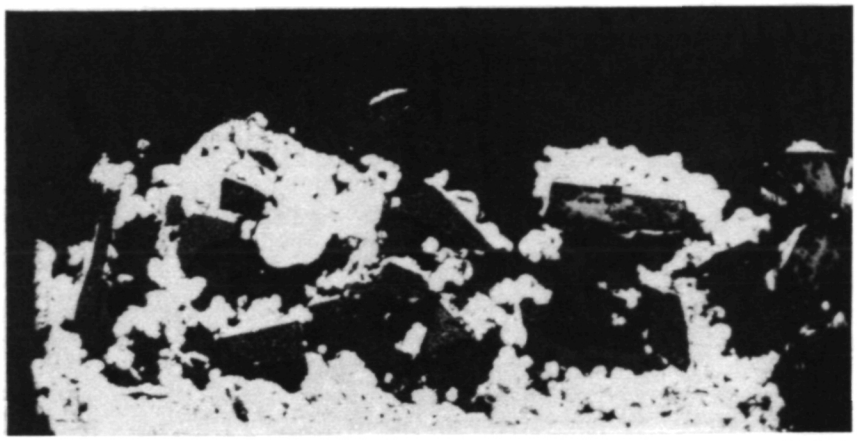

GRIT INJECTOR DISTANCE = 3.18 MM (100X)

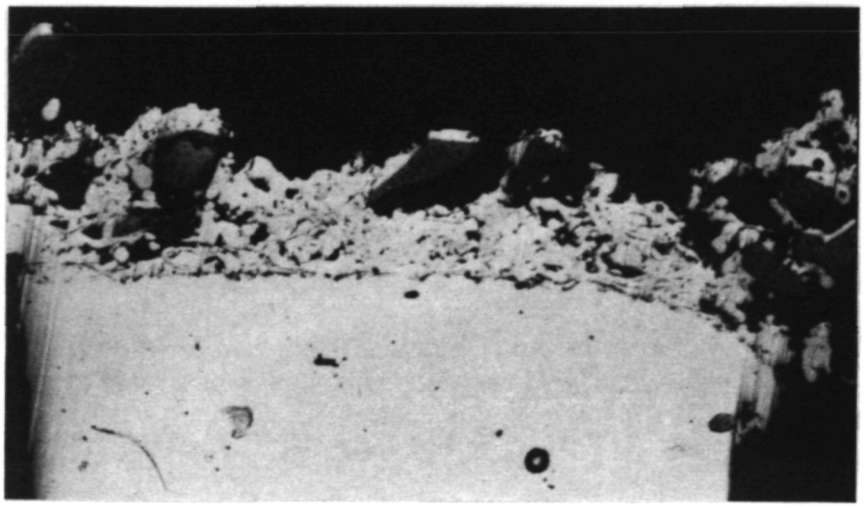

GRIT INJECTOR DISTANCE = 6.35 MM (100X)

Figure 3 Effects of Grit Injector-to-Substrate Distance on Grit Concentration.

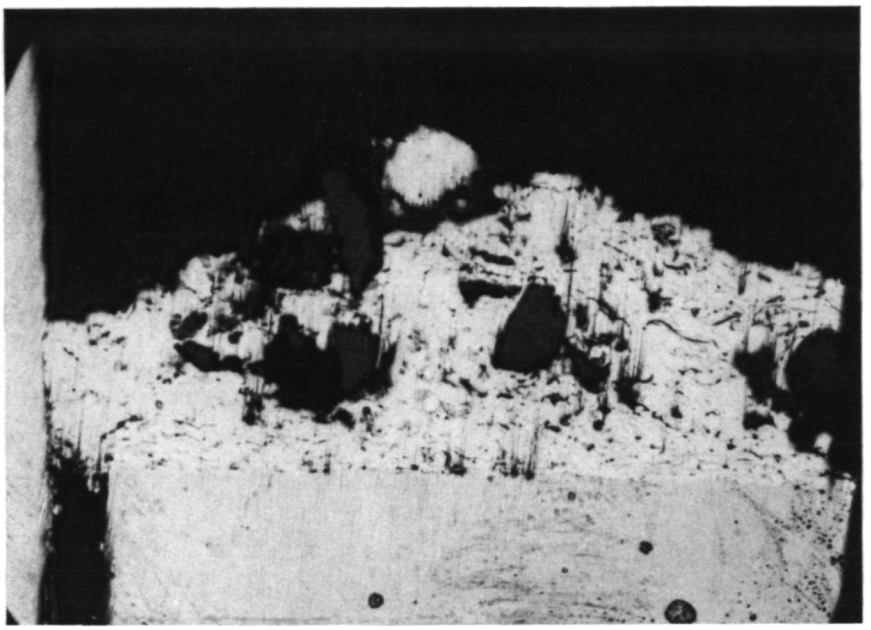

(100X)

PRIMARY ARC GAS FLOW = 3.68 M^3/HR

(100X)

PRIMARY ARC GAS FLOW = 2.83 M^3/HR

Figure 4 Effects of Primary Arc Gas Flow on Grit Concentration.

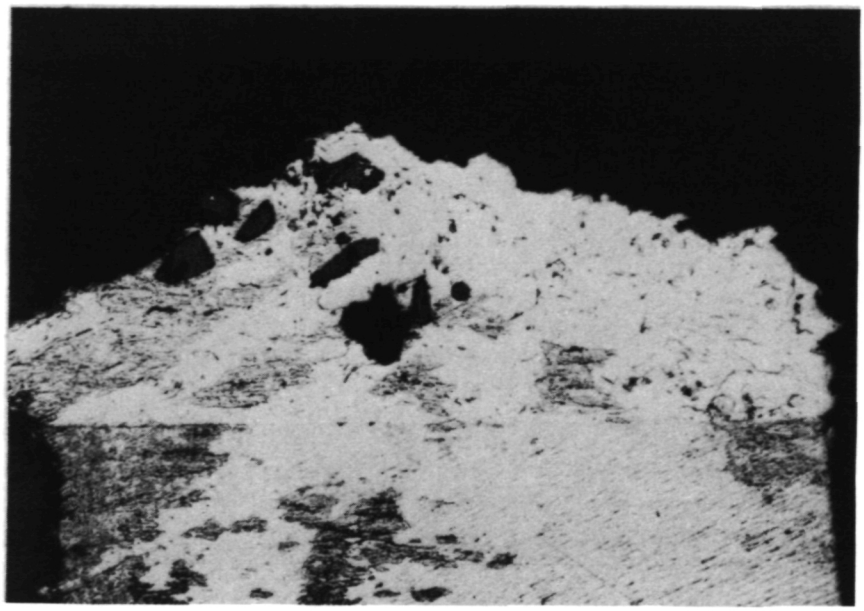

(100X)

AMPERAGE = 510

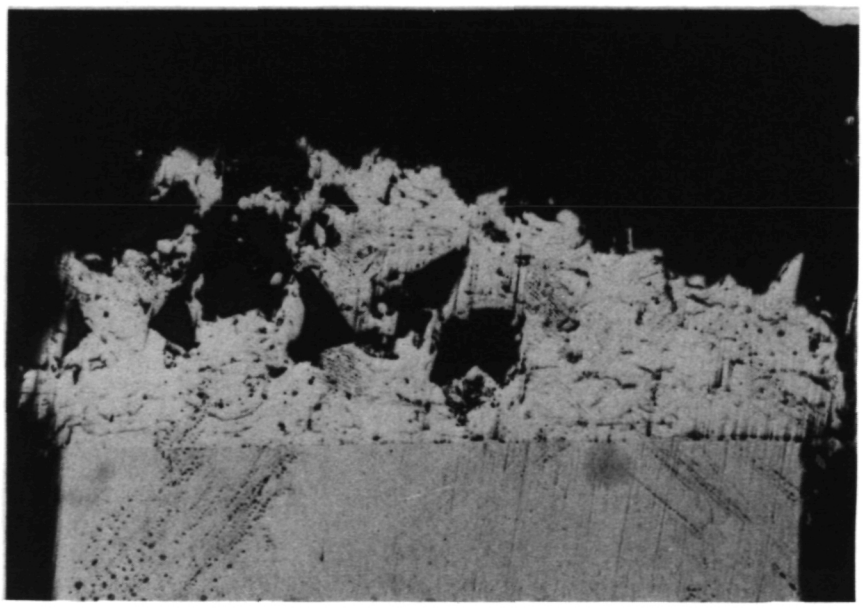

(100X)

AMPERAGE = 440

Figure 5 Effects of Plasma Gun Amperage on Grit Concentration.

The plasma spraying of abrasive grits becomes more difficult with increasing grit size due to the inherent self erosive character associated with large grits. Coating porosity increases, as well, due to the increased shadowing effect induced by the larger grits; Figure 6 compares the effects of No. 150, 0.05-0.12 mm, (0.002-0.005 inch) and No. 90, 0.12-0.20 mm (0.005-0.008 inch) size grits on coating porosity. In addition, as the grit size is increased, it becomes more difficult to produce acceptable coatings on thin 0.76 mm (0.030inch) thick compressor blade tips. This effect results from the increased tendency for self erosion by the large grits on the smaller target surface (tip cross section) coupled with the fact that there is proportionately less matrix volume available per grit which reduces the chance for grit capture. These grit size effects are depicted in Figure 7 for coatings with No. 150 and No. 54, 0.25-0.38 mm, (0.010-0.015 inch) grit sizes at approximately 25 percent grit concentration on 0.76 mm (0.030inch) thick tip cross sections.

To investigate the effect that target size has on grit capture, specimens with 2.54 mm (0.10 inch) thick cross sections were coated with No. 150 and No. 54 size grits in a METCO 443 matrix for comparison to coatings sprayed on 0.76 mm (0.030inch) thick specimens; as can clearly be seen in Figures 8 and 9, more grit capture is possible on 2.54 mm (0.10 inch) thick specimens than on 0.76 mm (0.030inch) thick specimens for both small and large grit sizes. Due to the difficulties in spraying large grits, only a limited number of 0.76 mm (0.030inch) thick blade specimens could be coated with No. 54 abrasive grits for rub testing.

After completing trial spraying to optimize spray parameters that would produce coatings consistent with the goals of the program, the final specimens were spray coated for test evaluation. The specimen substrate materials coated with the various matrix/abrasive grit material combinations, grit sizes, and the resulting average grit concentration levels obtained are shown in Table I. The average coating grit concentration is the average of the two specimens sprayed (one in the as-sprayed condition and the other after aging for 100 hours in air at 866°K temperature). The spray parameters optimized for the spraying of these test specimens also are listed in Table I and Table II lists the specifications of the plasma-spray equipment used. A sampling of the microsections representative of typical coatings produced are shown in Figures 10 through 22.

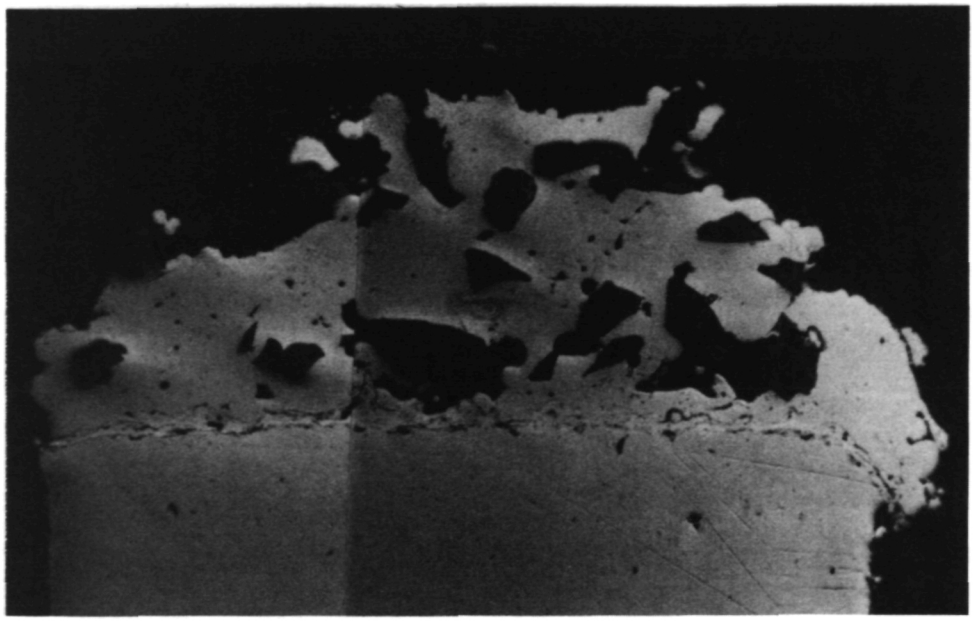

NO. 150 GRIT (100X)

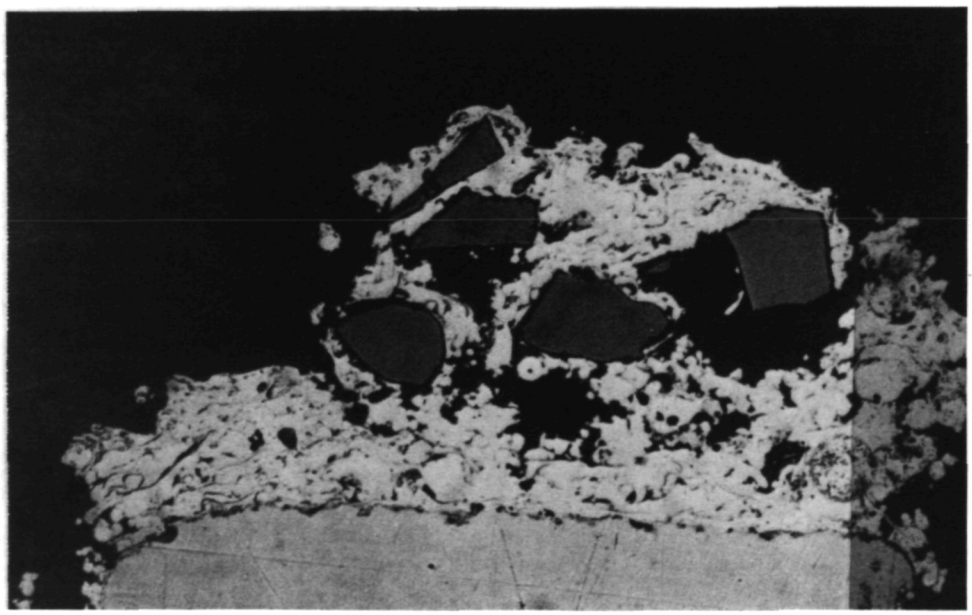

NO. 90 GRIT (100X)

Figure 6 Porosity Comparison of Coatings with No. 150 and No. 90 Size Grits.

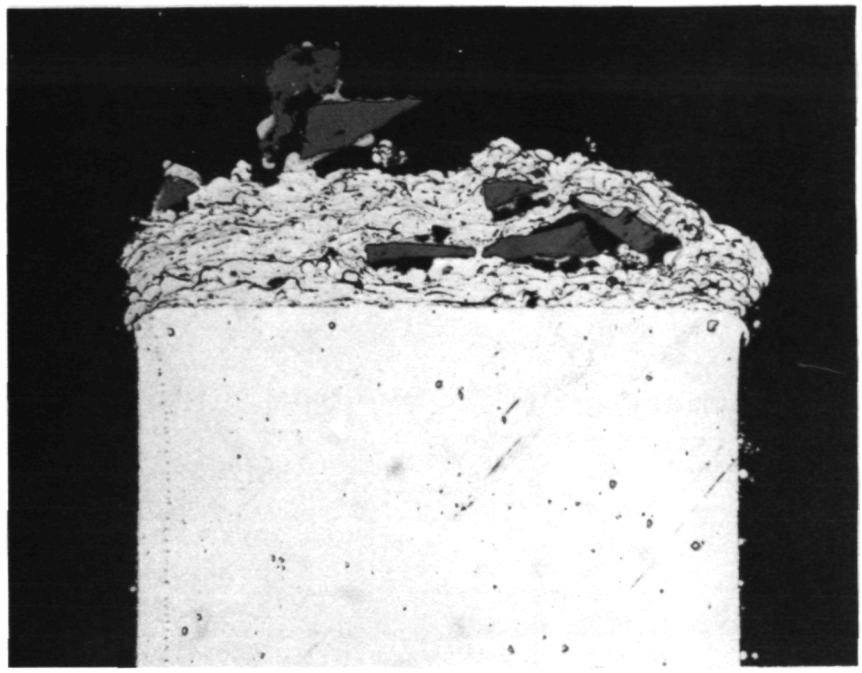

NO. 150 GRIT (100X)

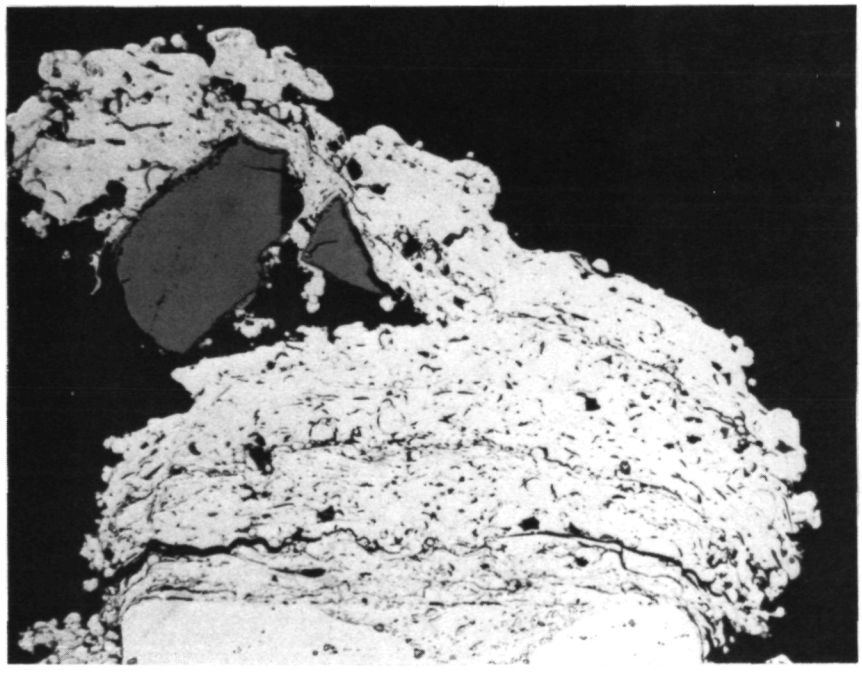

NO. 54 GRIT (100X)

Figure 7 Coating Comparisons with No. 150 and No. 54 Size Grits.

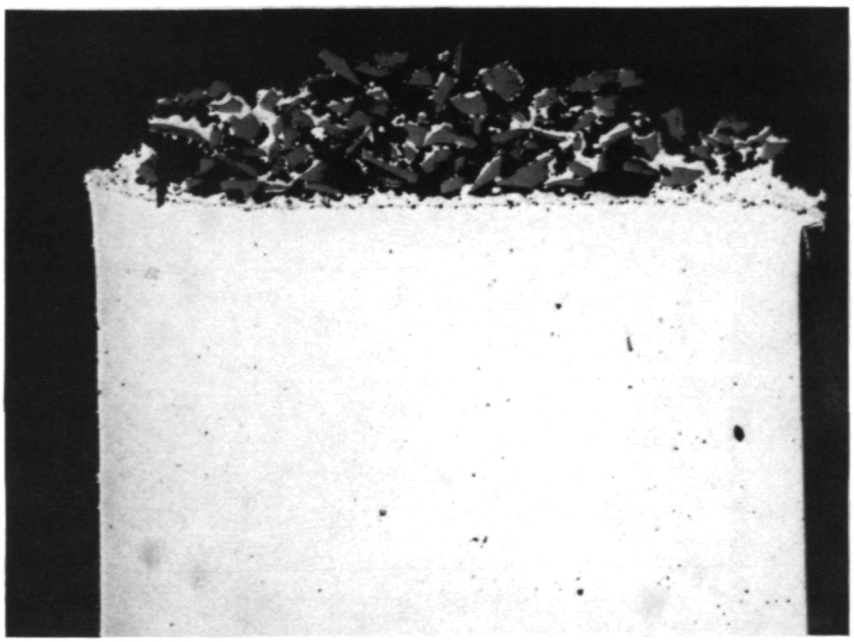

(40X)

NO. 150 SILICON CARBIDE GRIT ON 2.54 MM SUBSTRATE

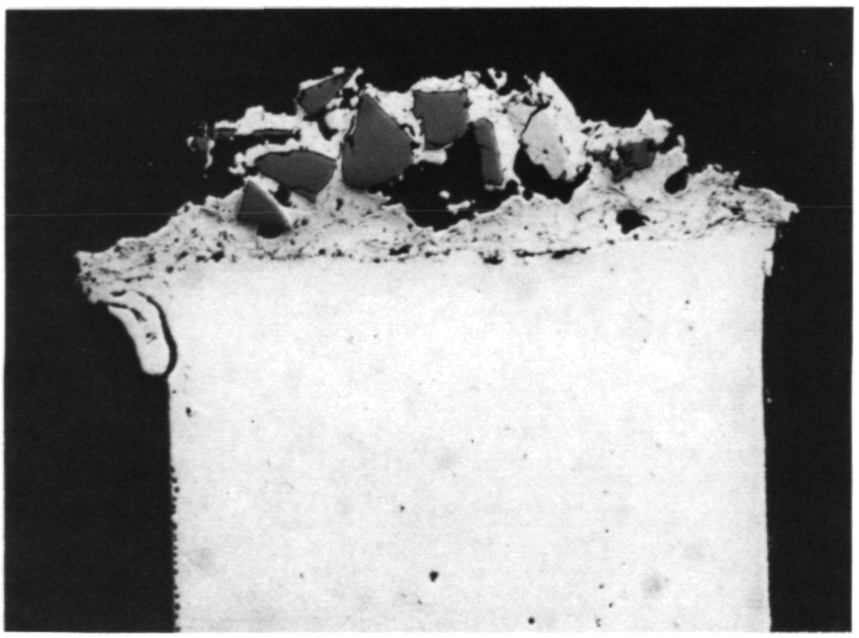

(100X)

NO. 150 SILICON CARBIDE GRIT ON 0.76 MM SUBSTRATE

Figure 8 Coatings with No. 150 Size Silicon Carbide (SiC) Grits on 0.76 and 2.54 mm Substrates.

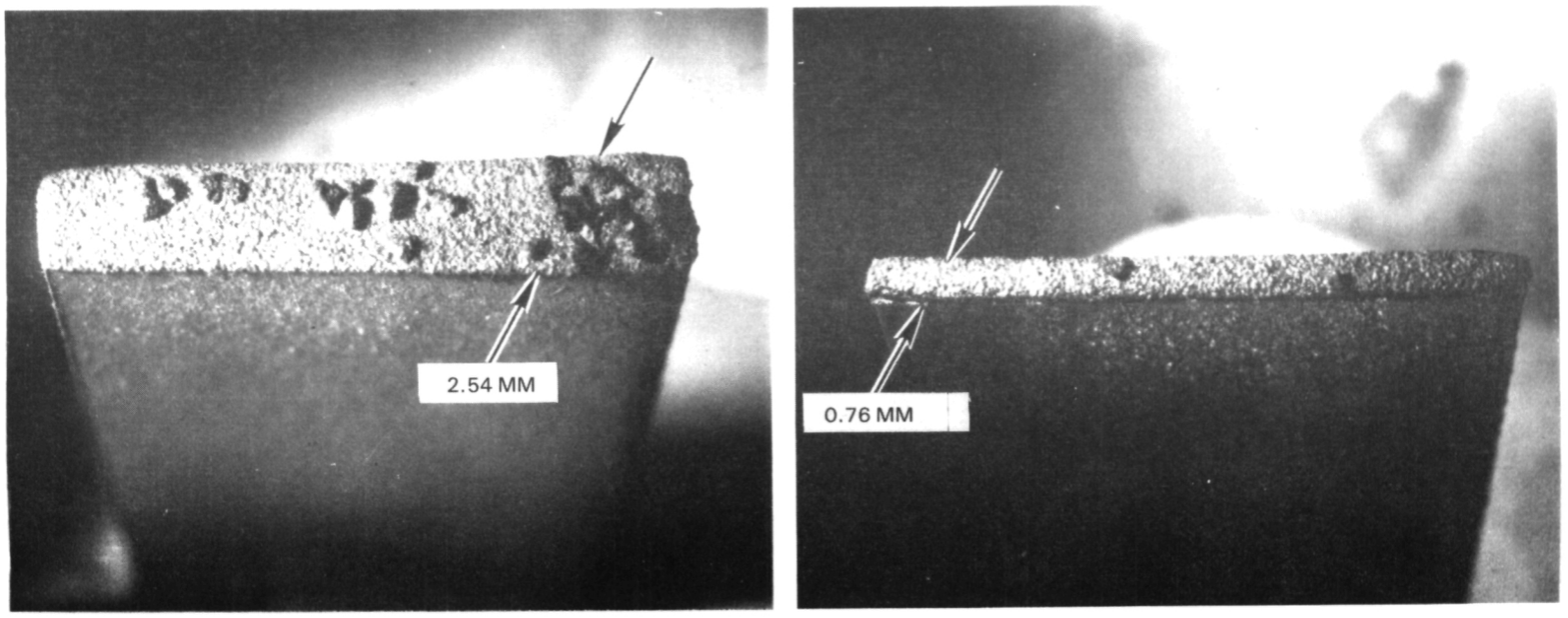

2.54 MM THICK BLADE TIP
NO. 54 GRIT

0.76 MM THICK BLADE TIP
NO. 54 GRIT

Figure 9 Coatings with No. 54 Size Silicon Carbide (SiC) Grits on 0.76 and 2.54 mm Substrates.

TABLE I

PLASMA-SPRAY PARAMETERS FOR CO-SPRAY SYSTEM

Matrix Material	Grit Material	Grit Size No.	Substrate Material	Target Grit Conc. %	Actual Grit Conc. Average %	Amps	Volts	Primary Gas Flow m3/hr (cfh)	Grit Injector to Substrate Distance mm (inches)	Grit Vibrator % of Full Scale	Spray Time Sec.	Fixture Rotation % of 180 rpm	Cooling Air Pressure N/cm^2 (psi)	Primary Arc Gas (N2) Pressure N/cm^2 (psi)	Secondary Arc*** Gas (H2) Pressure N/cm^2 (psi)	Matrix Carrier Gas (Ar) Flow m^3/hr (cfh)	Matrix Powder Feeder Speed (% of Full Scale)
Metco 443	SiC	150	Ti-6Al-4V	50	42	450	70	2.26 (80)	1.91 (0.075)	50	30	30	13.89 (20)	34.7 (50)	34.7 (50)	0.279 (9.9)	60
Metco 443	SiC	150	Ti-6Al-4V	25	17	550	70	2.26 (80)	1.91 (0.075)	50	23	25	13.89 (20)	34.7 (50)	34.7 (50)	0.279 (9.9)	60
Metco 443	Al_2O_3	150	Ti-6Al-4V	50	40	450	70	2.26 (80)	1.91 (0.075)	50	30	30	13.89 (20)	34.7 (50)	34.7 (50)	0.279 (9.9)	60
Metco 443	Al_2O_3	150	Ti-6Al-4V	25	25	550	70	2.26 (80)	1.91 (0.075)	50	23	25	13.89 (20)	34.7 (50)	34.7 (50)	0.279 (9.9)	60
Metco 43C	SiC	150	Ti-6Al-4V	50	37	300	70	1.70 (60)	1.91 (0.075)	50	20	30	13.89 (20)	34.7 (50)	34.7 (50)	0.279 (9.9)	60
Metco 43C	SiC	150	Ti-6Al-4V	25	16	400	70	2.26 (80)	1.91 (0.075)	50	20	30	13.89 (20)	34.7 (50)	34.7 (50)	0.279 (9.9)	60
Metco 43C	Al_2O_3	150	Ti-6Al-4V	50	23	300	70	1.70 (60)	1.91 (0.075)	50	20	30	13.89 (20)	34.7 (50)	34.7 (50)	0.279 (9.9)	60
Metco 43C	Al_2O_3	150	Ti-6Al-4V	25	30	400	70	2.26 (80)	1.91 (0.075)	50	20	30	13.89 (20)	34.7 (50)	34.7 (50)	0.279 (9.9)	60
Metco 16C	SiC	150	Ti-6Al-4V	50	38	400	70	1.84 (65)	1.91 (0.075)	50	20	30	13.89 (20)	34.7 (50)	34.7 (50)	0.279 (9.9)	60
Metco 16C	SiC	150	Ti-6Al-4V	25	18	480	70	2.26 (80)	1.91 (0.075)	50	20	30	13.89 (20)	34.7 (50)	34.7 (50)	0.279 (9.9)	60
Metco 16C	Al_2O_3	150	Ti-6Al-4V	50	47	400	70	2.12 (75)	1.91 (0.075)	50	20	30	13.89 (20)	34.7 (50)	34.7 (50)	0.279 (9.9)	60
Metco 16C	Al_2O_3	150	Ti-6Al-4V	25	31	450	70	1.98 (70)	1.91 (0.075)	50	20	30	13.89 (20)	34.7 (50)	34.7 (50)	0.279 (9.9)	60
Tribaloy 400	SiC	150	Ti-6Al-4V	50	37	300	70	1.70 (60)	1.91 (0.075)	50	20	30	13.89 (20)	34.7 (50)	34.7 (50)	0.279 (9.9)	60
Tribaloy 400	SiC	150	Ti-6Al-4V	25	26	350	70	2.26 (80)	1.91 (0.075)	50	20	30	13.89 (20)	34.7 (50)	34.7 (50)	0.279 (9.9)	60
Tribaloy 400	Al_2O_3	150	Ti-6Al-4V	50	39	350	70	2.26 (80)	1.91 (0.075)	50	20	30	13.89 (20)	34.7 (50)	34.7 (50)	0.279 (9.9)	60
Tribaloy 400	Al_2O_3	150	Ti-6Al-4V	25	6	400	70	2.26 (80)	1.91 (0.075)	50	20	30	13.89 (20)	34.7 (50)	34.7 (50)	0.279 (9.9)	60
Metco 443	SiC	90	Greek Ascoloy	25	32	500	70	1.98 (70)	1.91 (0.075)	30	35	15	13.89 (20)	34.7 (50)	34.7 (50)	0.249 (8.8)	80
Metco 443	SiC	90	Greek Ascoloy	10	9	400	70	1.98 (70)	1.91 (0.075)	30	35	15	13.89 (20)	34.7 (50)	34.7 (50)	0.249 (8.8)	80
Metco 443	SiC	90	Inconel 718	25	32	500	70	1.98 (70)	1.91 (0.075)	30	35	15	13.89 (20)	34.7 (50)	34.7 (50)	0.249 (8.8)	80
Metco 443	SiC	90	Inconel 718	10	9	400	70	1.98 (70)	1.91 (0.075)	30	35	15	13.89 (20)	34.7 (50)	34.7 (50)	0.249 (8.8)	80
Metco 443	SiC	90	Ti-6Al-4V	25	32	500	70	1.98 (70)	1.91 (0.075)	30	35	15	13.89 (20)	34.7 (50)	34.7 (50)	0.249 (8.8)	80
Metco 443	SiC	90	Ti-6Al-4V	10	9	400	70	1.98 (70)	1.91 (0.075)	30	35	15	13.89 (20)	34.7 (50)	34.7 (50)	0.249 (8.8)	80
Metco 443	SiC	150	Inconel 718	30-40	25	550	70	2.12 (75)	1.78 (0.070)	60	20	20	6.94 (10)	34.7 (50)	34.7 (50)	0.249 (8.8)	80
Metco 443	SiC	150	Inconel 718	15-25	23	600	70	2.83 (100)	1.78 (0.070)	40	15	30	6.94 (10)	34.7 (50)	34.7 (50)	0.249 (8.8)	80
Metco 443	Si_3N_4	150	Inconel 718	30-40	39	500	70	2.12 (75)	1.78 (0.070)	60	25	20	6.94 (10)	34.7 (50)	34.7 (50)	0.249 (8.8)	100
Metco 443	Si_3N_4	150	Inconel 718	15-25	22	550	70	2.12 (75)	1.78 (0.070)	60	25	20	6.94 (10)	34.7 (50)	34.7 (50)	0.249 (8.8)	100
Tipaloy	SiC	150	Inconel 718	30-40	35	550	70	2.12 (75)	1.78 (0.070)	60	20	20	6.94 (10)	34.7 (50)	34.7 (50)	0.249 (8.8)	80
Tipaloy	SiC	150	Inconel 718	15-25	20	550	70	2.83 (100)	1.78 (0.070)	40	15	30	6.94 (10)	34.7 (50)	34.7 (50)	0.249 (8.8)	80
Tipaloy	Si_3N_4	150	Inconel 718	30-40	30	500	70	2.12 (75)	1.78 (0.070)	60	25	20	6.94 (10)	34.7 (50)	34.7 (50)	0.218 (7.7)	100
Metco 443	Si_3N_4	150	Inconel 718	15-25	12	550	70	2.12 (75)	1.78 (0.070)	60	25	20	6.94 (10)	34.7 (50)	34.7 (50)	0.218 (7.7)	100
Metco 443	SiC	54	Inconel 718	10-15	--	450	65	2.12 (75)	1.78 (0.070)	30	2 Passes**	3.8*	6.94 (10)	34.7 (50)	34.7 (50)	0.230 (8.14)	100
Tipaloy	SiC	54	Inconel 718	20-25	--	450	65	2.12 (75)	1.78 (0.070)	30	2 Passes**	4.45*	6.94 (10)	34.7 (50)	34.7 (50)	0.230 (8.14)	100
Tipaloy	SiC	54	Inconel 718	10-15	--	450	65	2.12 (75)	1.78 (0.070)	30	1 Pass**	4.45*	6.94 (10)	34.7 (50)	34.7 (50)	0.230 (8.14)	100
Tipaloy	Si_3N_4	54	Inconel 718	10-15	--	450	65	2.12 (75)	1.78 (0.070)	30	2 Passes**	3.8*	6.94 (10)	34.7 (50)	34.7 (50)	0.230 (8.14)	100

*No fixture rotation; spray gun was translated across specimen at these rates in cm/sec.
**Number of spray gun passes to obtain coating thickness
***Secondary arc gas (H2) flow adjusted to obtain voltage

Plasma gun distance 6.03 cm (2.375 inches)
Cooling air jet distance 5.08 cm (2.0 inches) Grit carrier gas flow (Ar) 0.566 m^3/hr (20 cfh)

TABLE II

SPECIFICATIONS OF PLASMA-SPRAY EQUIPMENT

Plasma-Spray System:

Name: Metco 7M Spray System	
Manufactured By: Metco, Inc., Westbury L.I., N.Y.	
Spray Gun	7MB
Nozzle	G
Powder Feeder Meter Wheel	P
Powder Port No.	2
Power Supply	6 MR
Control Unit	6 MC
Powder Feeder	3 MP
Horizontal-Vertical Transverse Unit	4HC
Rotating Turntable Unit	3H7
Flame Spray Booth	4 BWH

Grit Powder Feed System:

Name: Thermal Arc Model P1-200-2 Ser. No. 6439
Manufactured By: Sylvester & Co., Cleveland, Ohio
Injector Tube Diameter: 6.35 mm (0.25 inch)

(100X)

36% GRIT CONCENTRATION

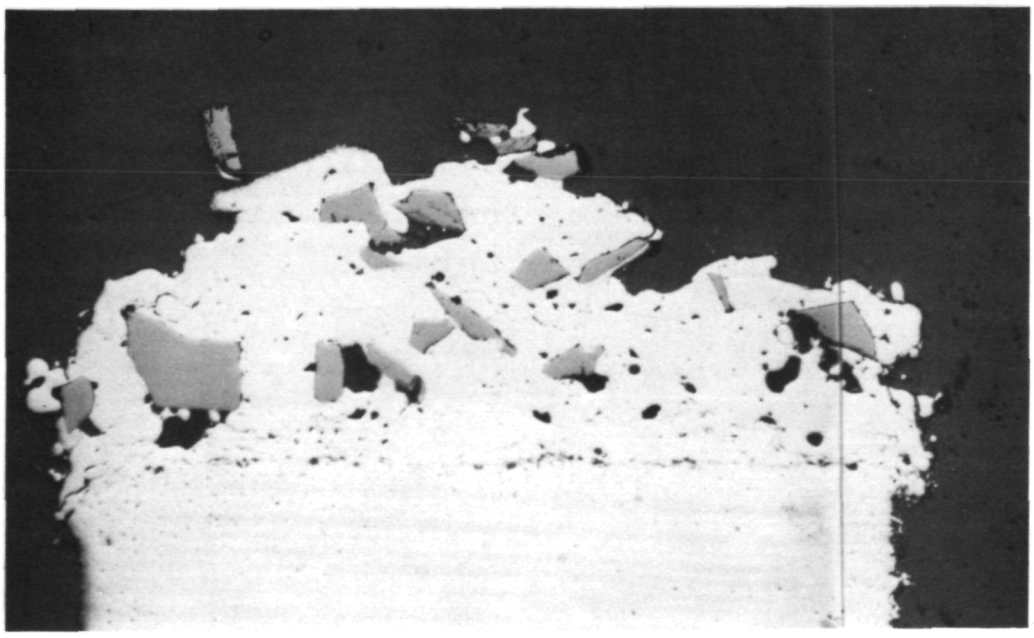

(100X)

21% GRIT CONCENTRATION

Figure 10 METCO 16C with No. 150 Size Silicon Carbide (SiC) Grits at 21 and 36 percent Grit Concentrations.

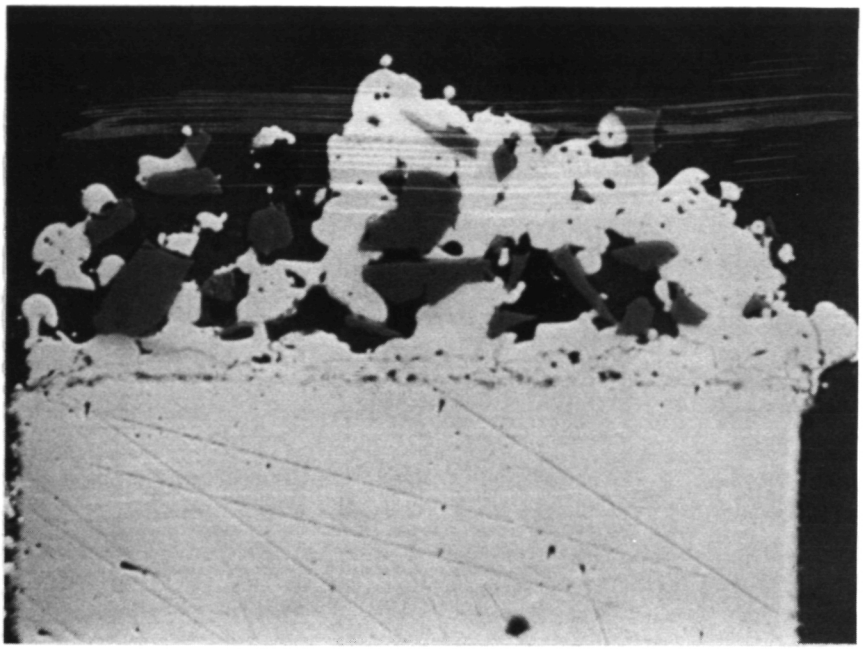

(100X)

57% GRIT CONCENTRATION

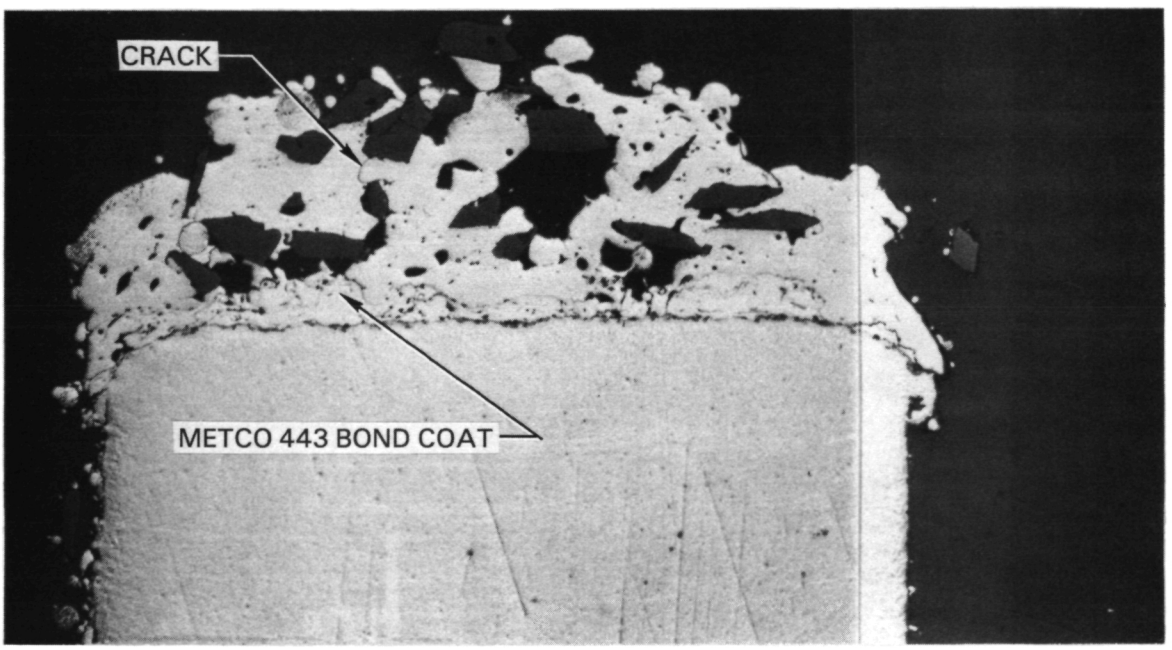

(100X)

35% GRIT CONCENTRATION

Figure 11 METCO 16C with No. 150 Size Aluminum Oxide (Al_2O_3) Grits at 35 and 57 percent Grit Concentrations.

(100X)

43% GRIT CONCENTRATION

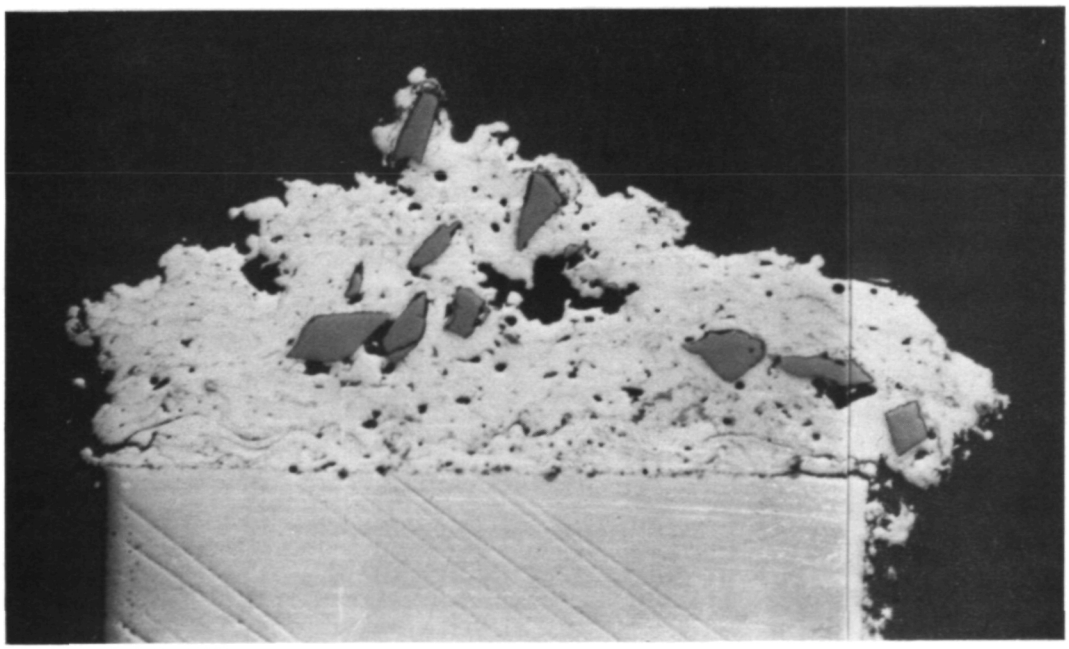

(100X)

19% GRIT CONCENTRATION

Figure 12 METCO 43C with No. 150 Size Silicon Carbide (SiC) Grits at 19 and 43 percent Grit Concentrations.

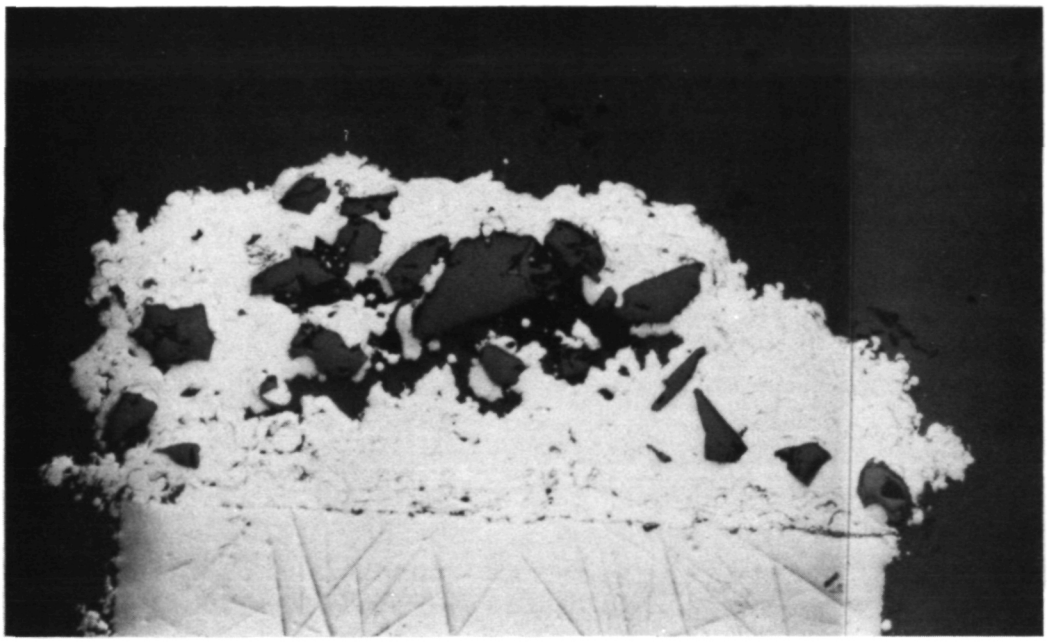

(100X)

32% GRIT CONCENTRATION

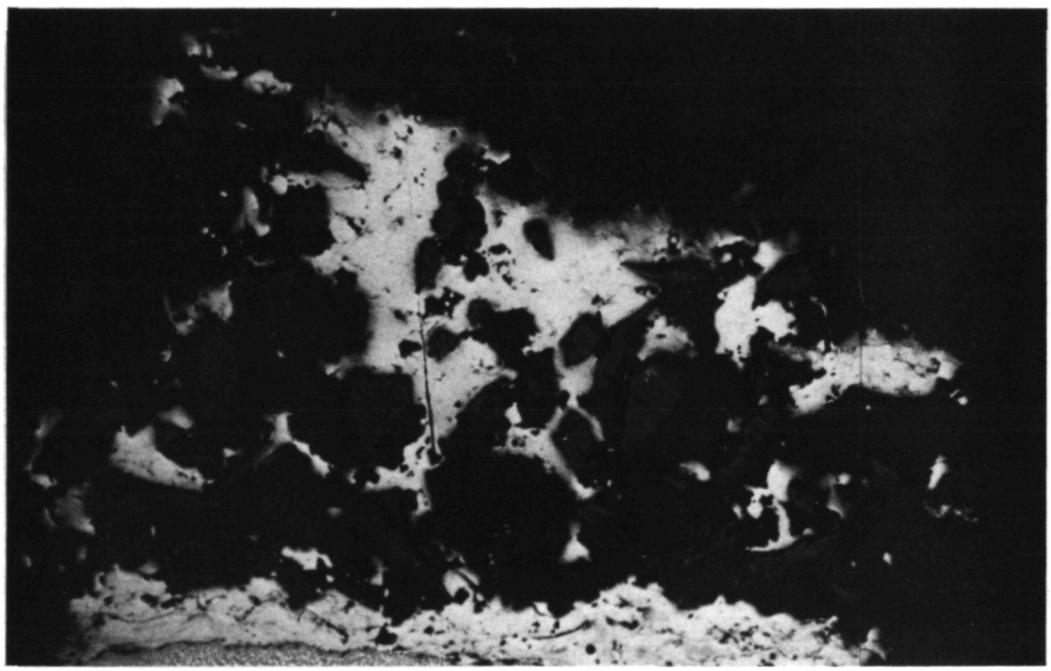

(100X)

29% GRIT CONCENTRATION

Figure 13 METCO 43C with No. 150 Size Aluminum Oxide (Al_2O_3) Grits at 29 and 32 percent Grit Concentrations.

(100X)

52% GRIT CONCENTRATION

(100X)

25% GRIT CONCENTRATION

Figure 14 METCO 443 with No. 150 Size Silicon Carbide (SiC) Grits at 25 and 50 percent Grit Concentrations.

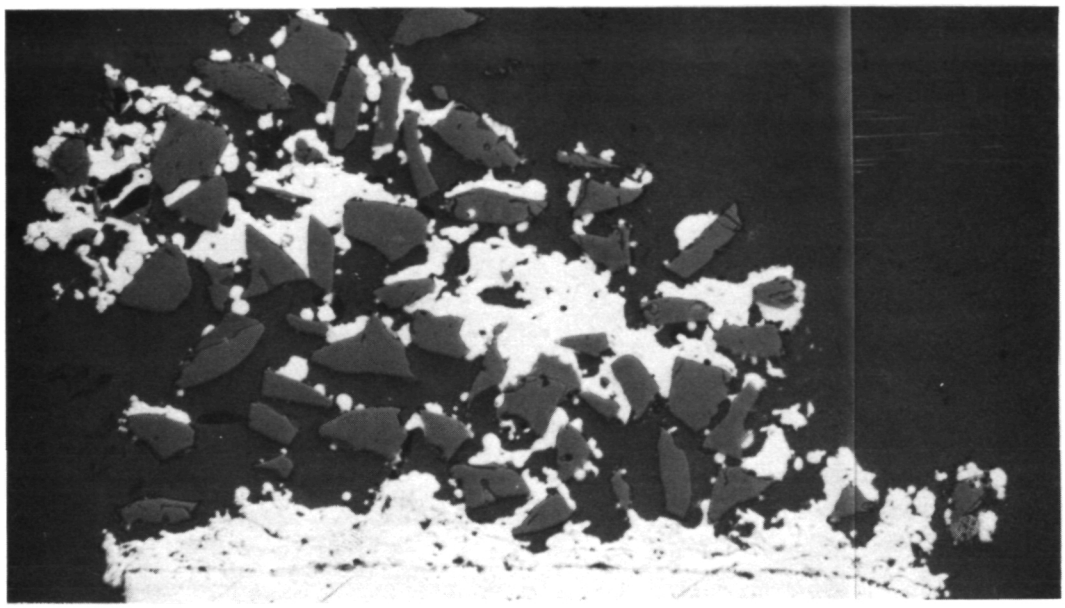

(100X)

53% GRIT CONCENTRATION

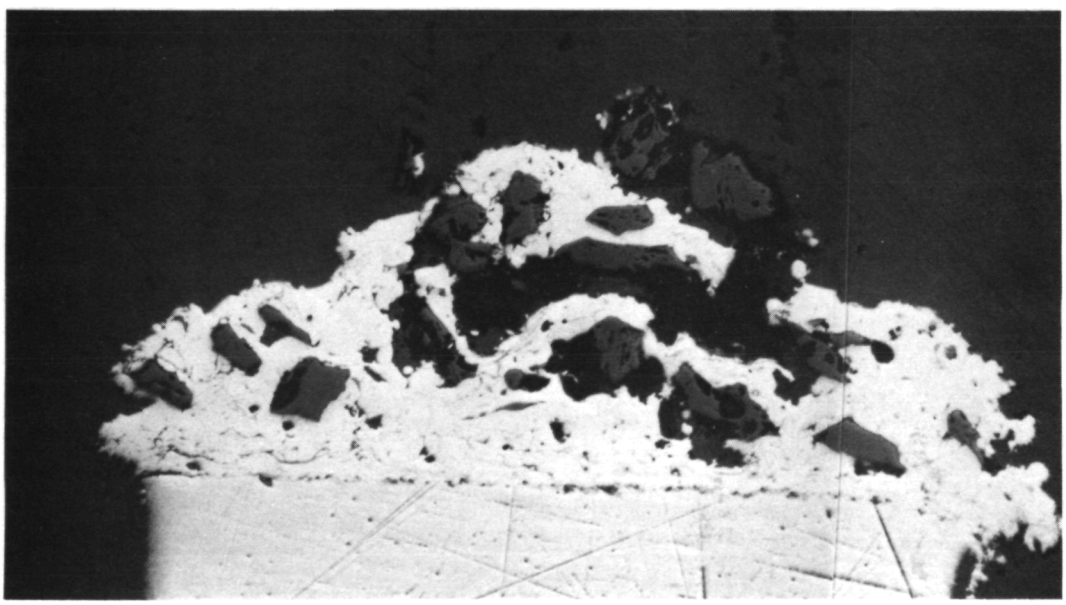

(100X)

30% GRIT CONCENTRATION

Figure 15 METCO 443 with No. 150 Size Aluminum Oxide (Al_2O_3) Grits at 30 and 53 percent Grit Concentrations.

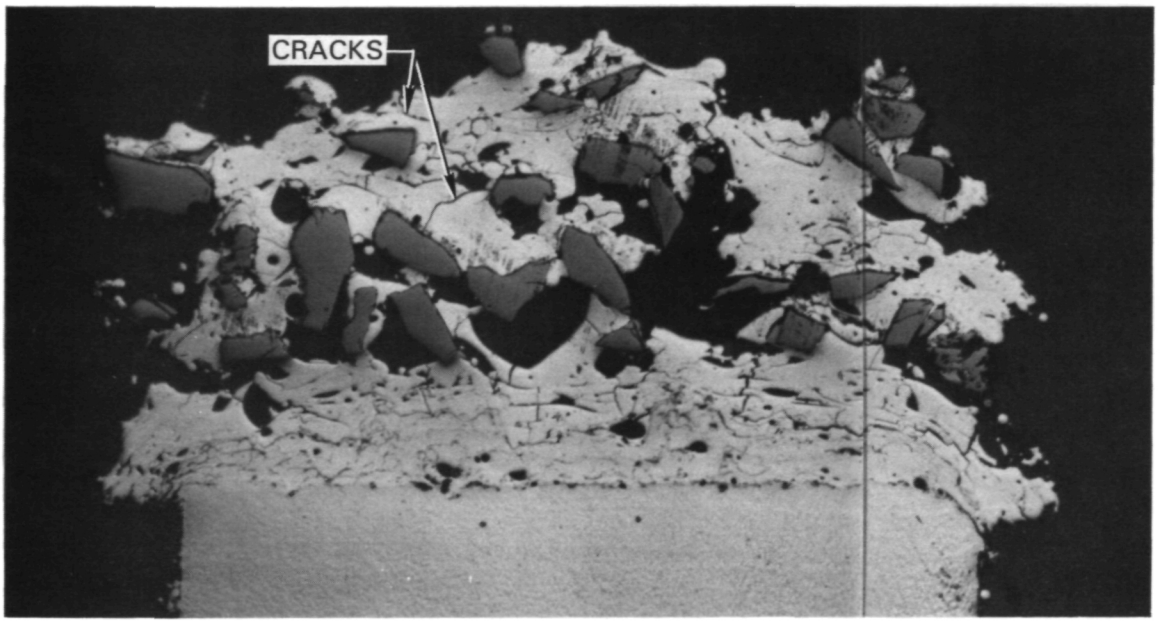

(100X)

41% GRIT CONCENTRATION

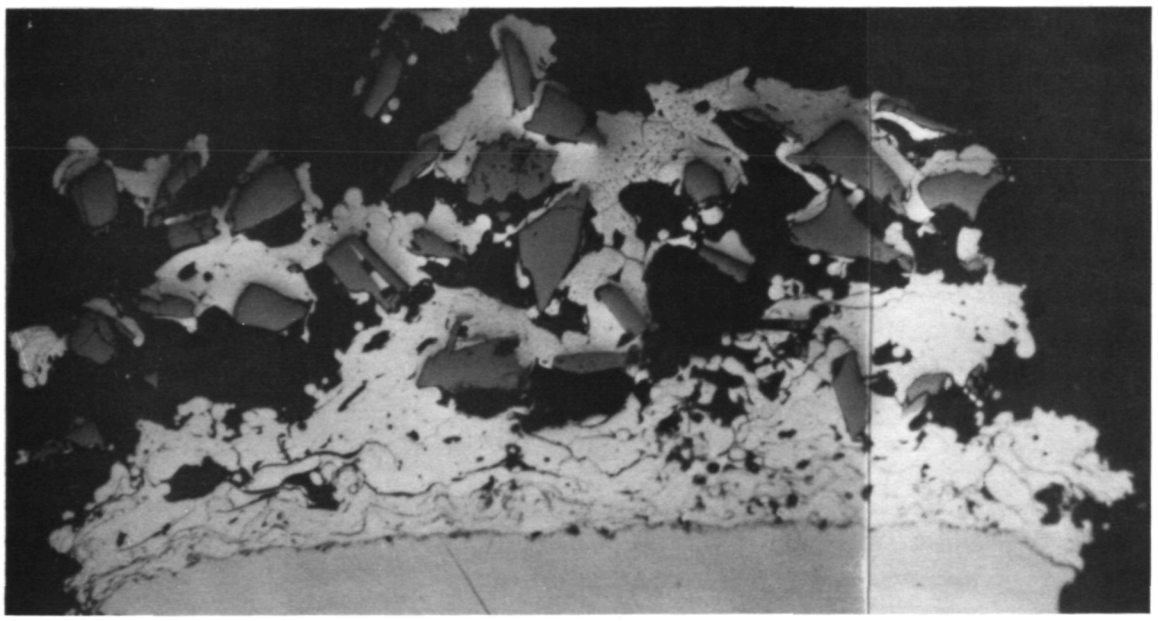

(100X)

27% GRIT CONCENTRATION

Figure 16 TRIBALOY 400 with No. 150 Size Silicon Carbide (SiC) Grits at 27 and 41 percent Grit Concentrations.

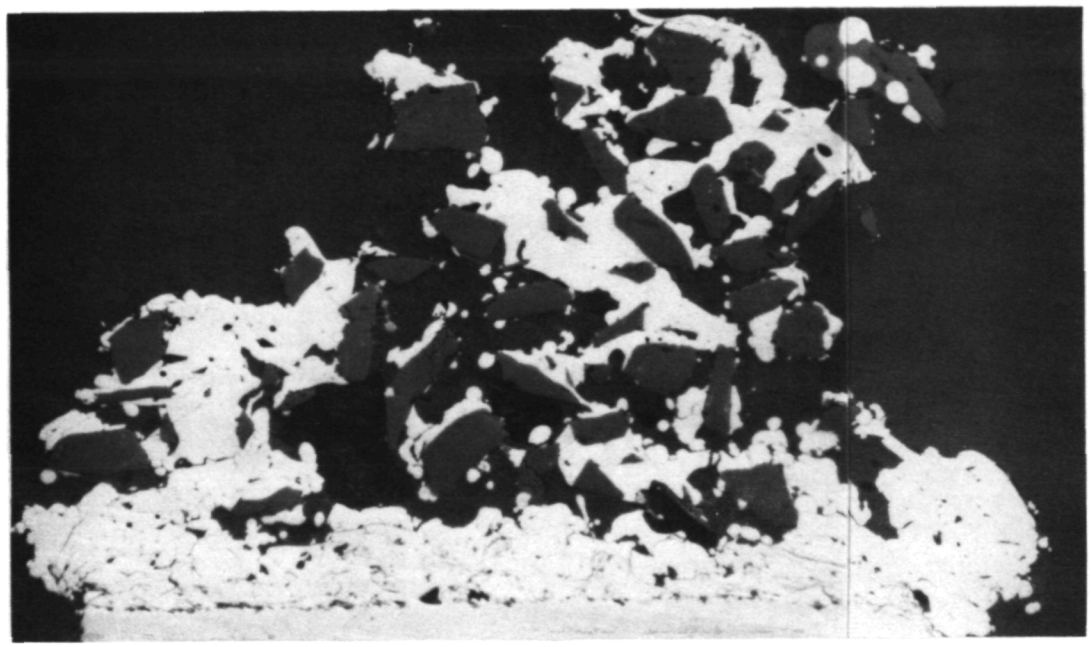

(100X)

49% GRIT CONCENTRATION

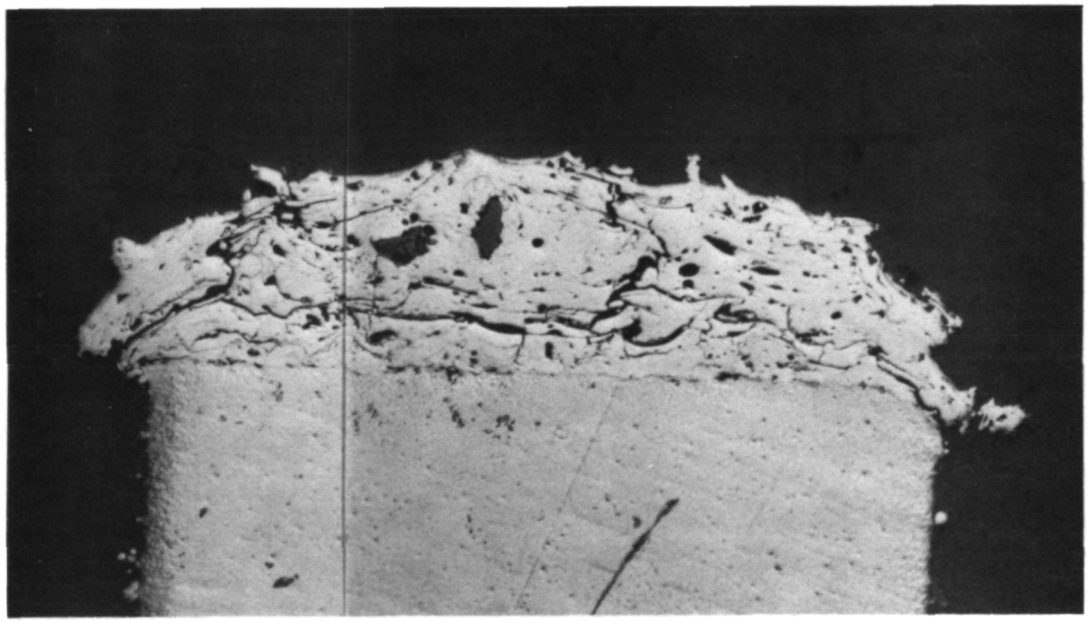

(100X)

5% GRIT CONCENTRATION

Figure 17 TRIBALOY 400 with No. 150 Size Aluminum Oxide (Al_2O_3) Grits at 5 and 49 percent Grit Concentrations.

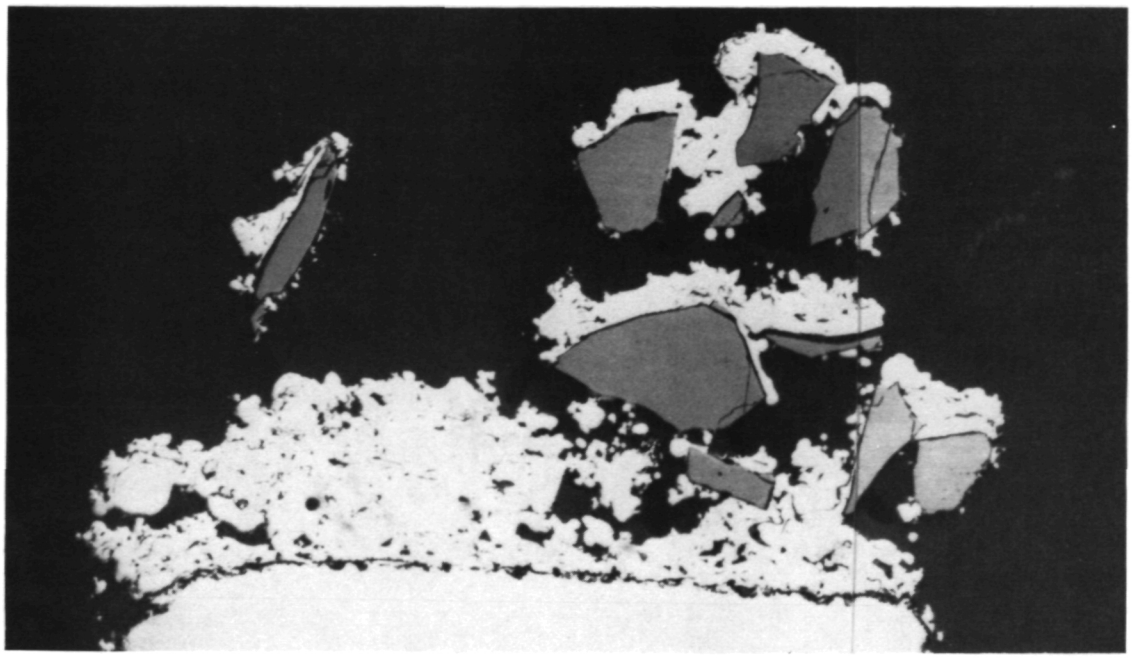

(100X)

27% GRIT CONCENTRATION

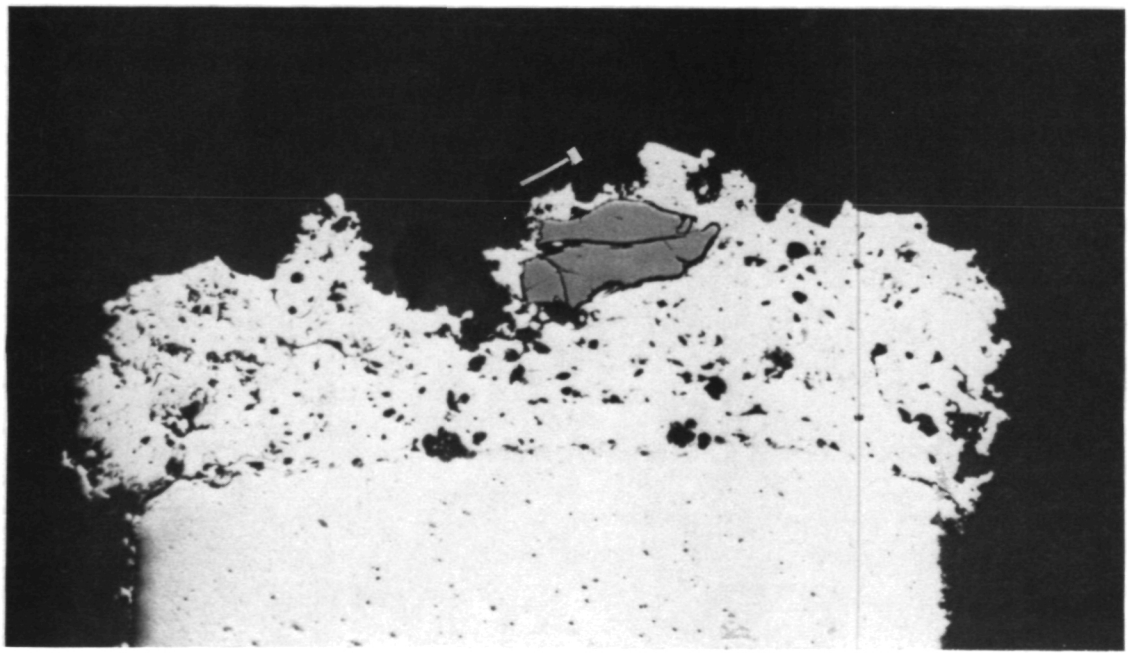

(100X)

10% GRIT CONCENTRATION

Figure 18 METCO 443 with No. 90 Size Silicon Carbide (SiC) Grits at 10 and 27 percent Grit Concentrations.

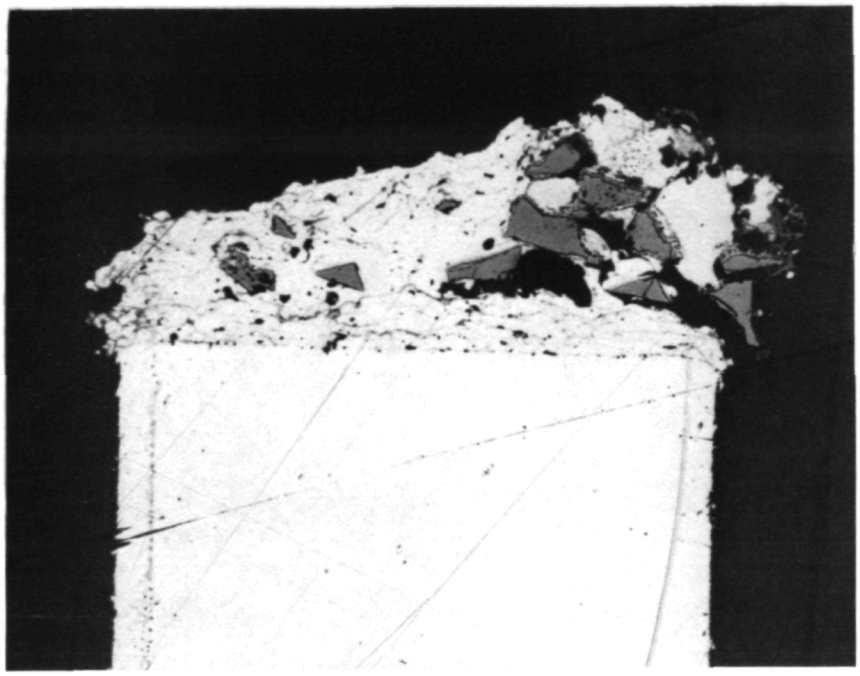

(100X)

31% GRIT CONCENTRATION

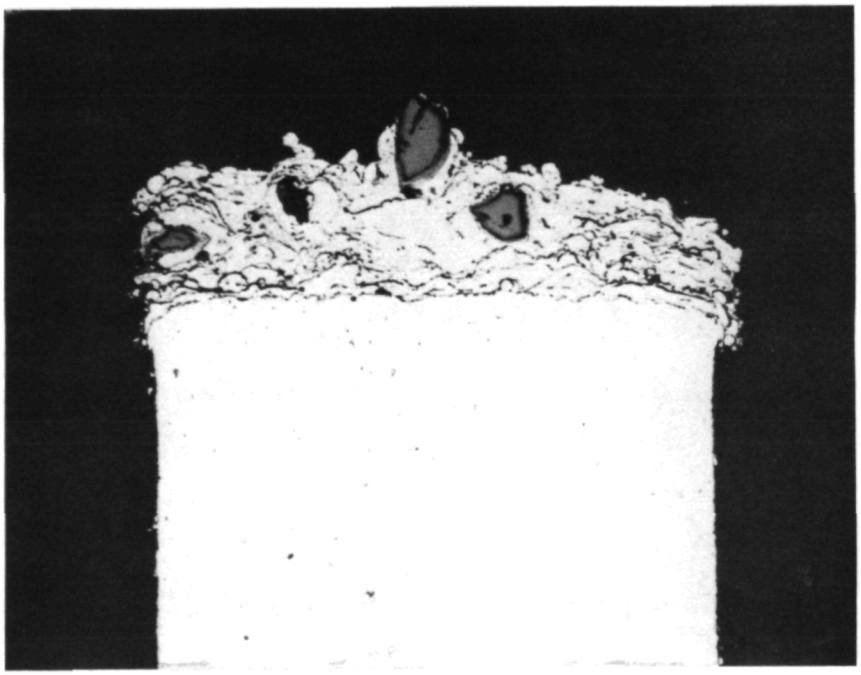

(100X)

18% GRIT CONCENTRATION

Figure 19 METCO 443 with No. 150 Size Silicon Carbide (SiC) Grits at 18 and 31 percent Grit Concentrations.

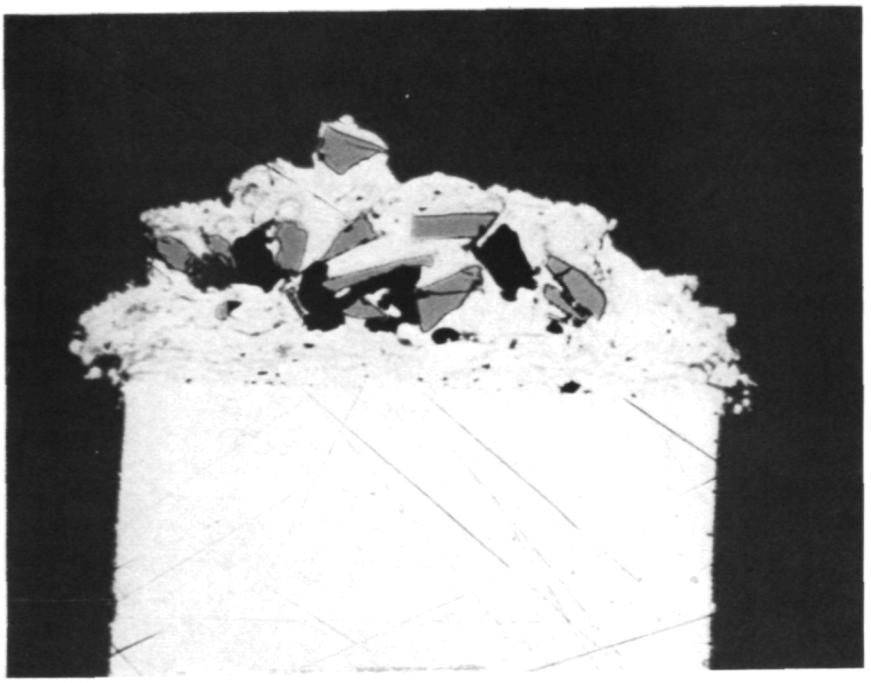

(100X)

31% GRIT CONCENTRATION

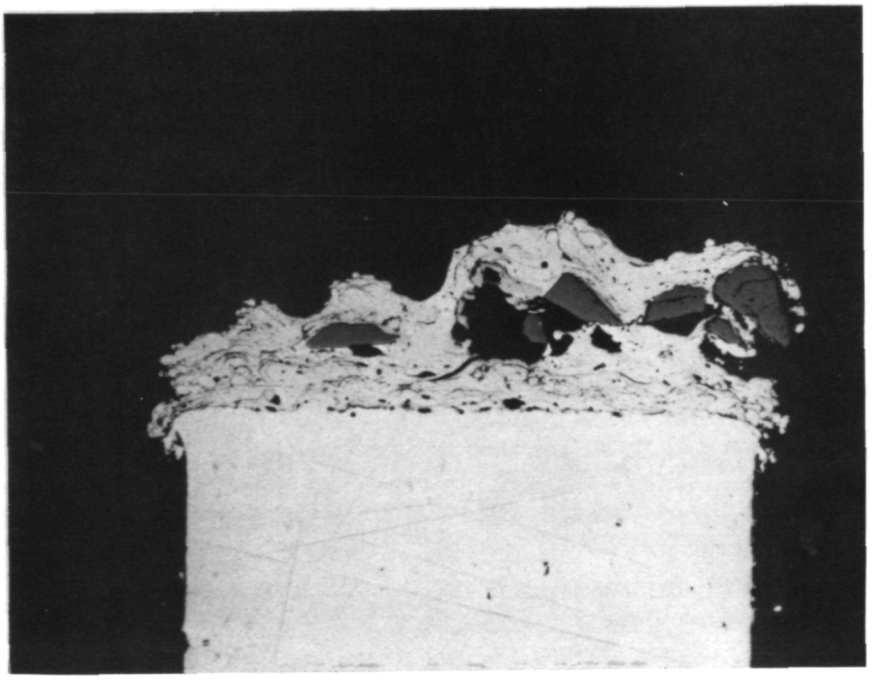

(100X)

24% GRIT CONCENTRATION

Figure 20 TIPALOY with No. 150 Size Silicon Carbide (SiC) Grits at 24 and 31 percent Grit Concentrations.

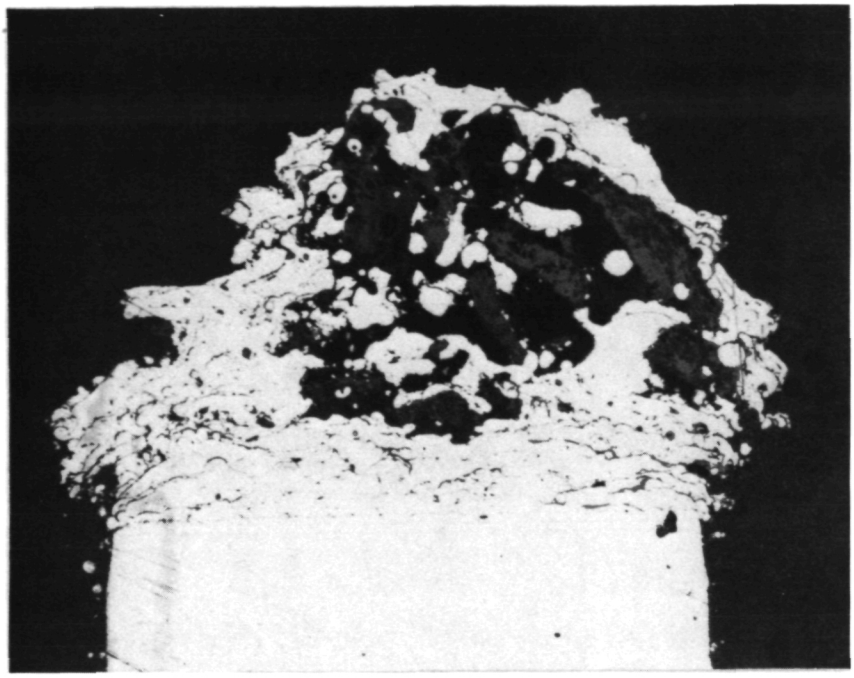

(100X)

35% GRIT CONCENTRATION

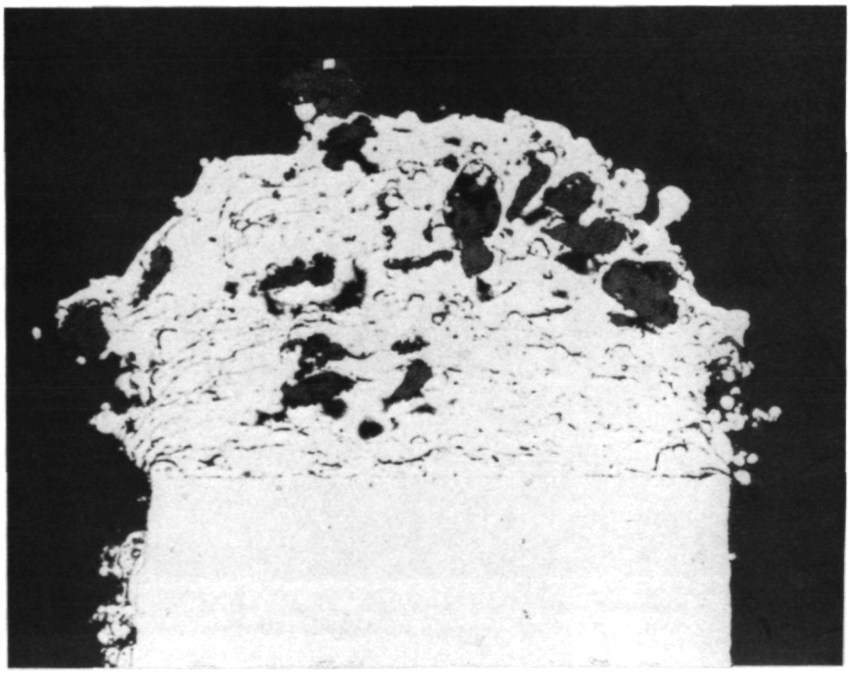

(100X)

19% GRIT CONCENTRATION

Figure 21 METCO 443 with No. 150 Size Silicon Nitride (Si_3N_4) Grits at 19 and 35 percent Grit Concentrations.

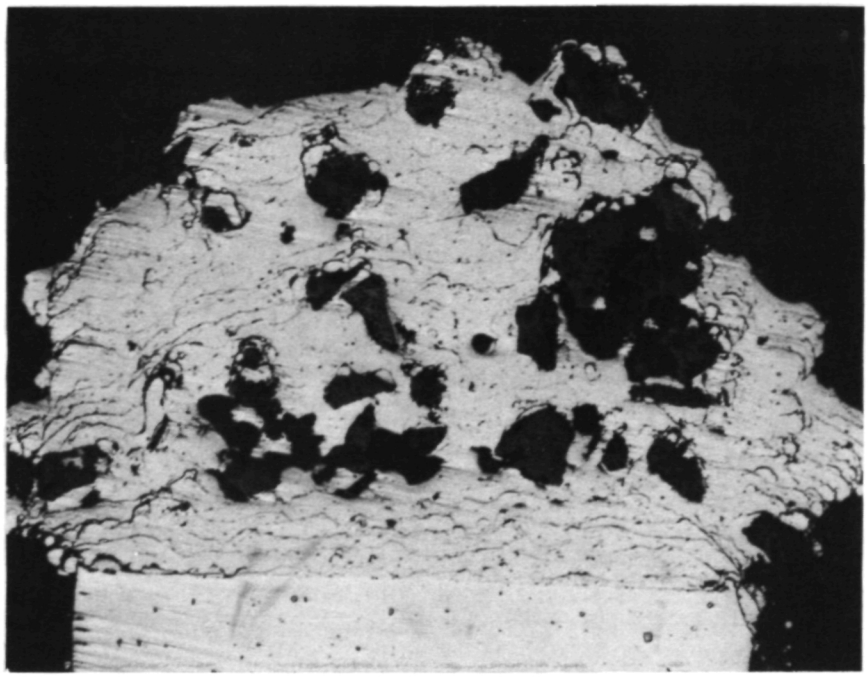

(100X)

28% GRIT CONCENTRATION

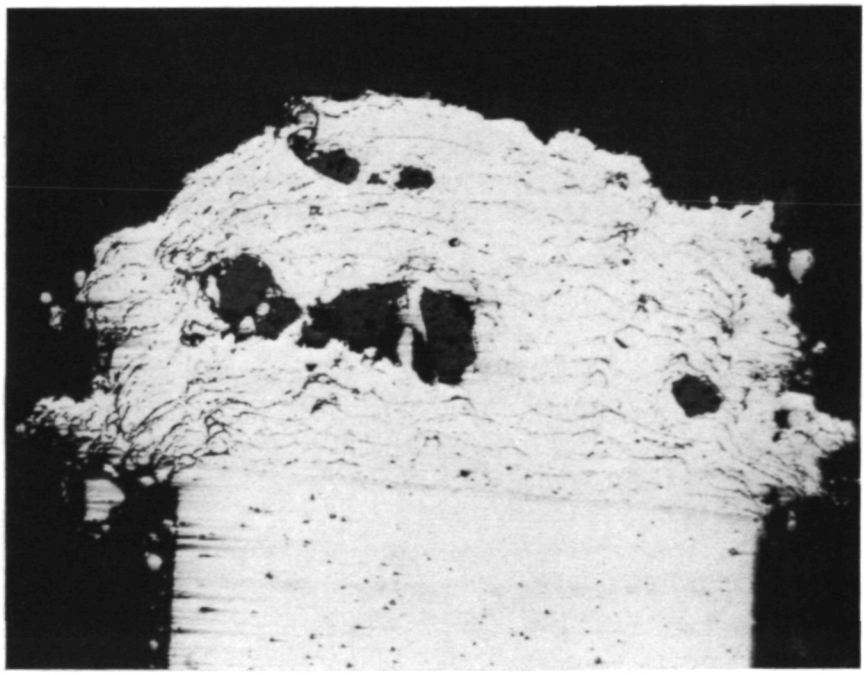

(100X)

15% GRIT CONCENTRATION

Figure 22 TIPALOY with No. 150 Size Silicon Nitride (Si_3N_4) Grits at 15 and 28 percent Grit Concentrations.

Sufficient specimens were coated for conducting bond adherence, erosion, and rub tests and for performing microscopic examinations on each of the coating combinations in the as-sprayed condition and after aging for 100 hours at 866K (1100°F) temperature in air. Figure 23 shows the specimen substrates that were coated for test evaluation; these test specimens are described below:

- Rub test specimens - small scale simulated compressor blades having 0.76 mm (0.030 inch) x 6.35 mm (0.25 inch) tip cross sections with a dovetail for mounting in a rotating disk.

- Erosion specimens - 20.3 mm (0.80 inch) x 20.3 mm (0.80 inch) square by 20.9 mm (0.90 inch) thick flats fabricated from sheet metal stock.

- Bond adhesion specimens - standard 25.4 mm (1.0 inch) diameter tensile specimens with a threaded end for mounting in a tensile testing machine.

- Microscopic examination specimens - 19.1 mm (0.75 inch) long sheet metal strips with 0.76 mm (0.030 inch) x 6.35 mm (0.25 inch) tip cross sections, representative of the rub specimen tips.

Since it was not within the scope of the program to adjust spray parameters to account for the effect that the larger target areas of the erosion and adhesion specimens may have on spray deposition, these specimens were prepared using the identical parameters that were determined for the blade rub test specimens. The only exception was that the plasma gun was traversed across the specimens as they rotated through the plasma stream to accommodate coating of the larger specimen width.

3.3 EXPERIMENTAL EVALUATION

3.3.1 Microscopic Examination

Microscopic examinations were conducted on each candidate matrix/abrasive grit coating combination to determine the actual abrasive grit volumetric concentration, the size and shape of the abrasive grits in the coating and the extent of compositional and morphological changes caused by aging. The coatings were also examined to determine if any interactions had occurred between the matrix, abrasive grits, and the substrate during the spray process.

The specimens were prepared by impregnating them under vacuum with Stycast^{R} followed by carefully polishing for microscopic examination. A "Leitz Metalloplan 500" with Polaroid camera, Figure 24, was used for observation and photographic documentation of each abrasive coating evaluated.

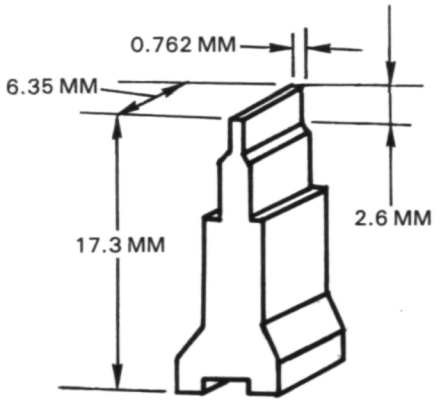

SIMULATED COMPRESSOR BLADE
RUB SPECIMEN

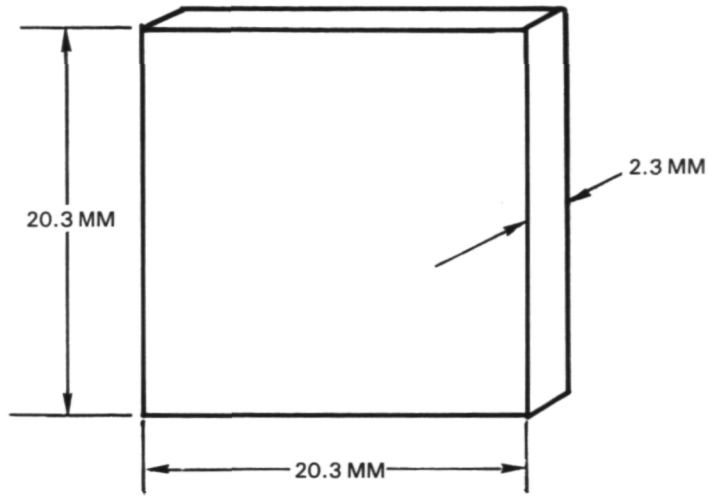

EROSION SPECIMEN

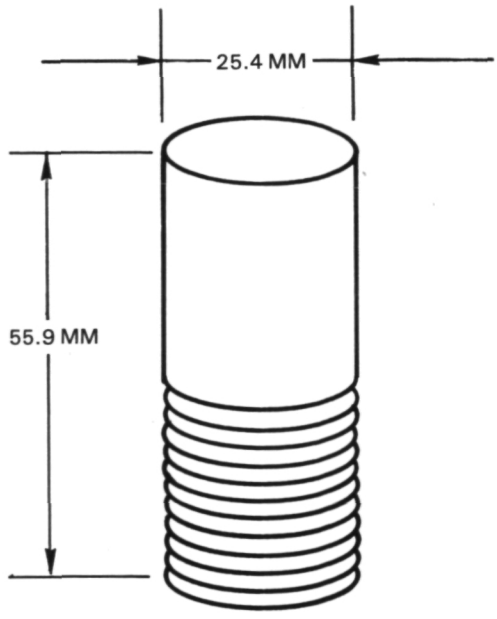

ADHESION SPECIMEN

Figure 23 Specimens Sprayed for Rub, Erosion, and Adhesion Tests.

Figure 24 Leitz Metalloplan "500" Metallograph with Polaroid Camera.

The abrasive grit volumetric percent concentration was determined using transparent paper with a grid network of 1.27 mm (0.05 inch) square placed over a 100X microphotograph of the coating and counting the grid line intersections bounded by the grits and dividing by the total number of grid line intersections bounded by the entire coating.

This is not an exact method for determining grit concentration; however, the development of an alternate method, such as dissolution, was beyond the scope of the program. A series of measurements taken of 18 coatings comparing several microsection slices both normal and parallel to the surface indicate, at best, that concentration levels could only be categorized in low (10 to 20 percent), medium (20 to 30 percent), or high (30 to 50 percent) ranges. This also is approximately the same accuracy capability expected by the plasma "co-spray" process used to apply the coatings.

Each coating was microscopically examined in the as-sprayed condition and after aging for 100 hours at 866K (1100°F) temperature in air. The results of these examinations are as follows:

Abrasive Grits

Silicon carbide - Retains its sharp angular unmelted shape in combination with all metal matrices. After aging for 100 hours at 866K (1100°F) temperature in air, a limited amount of reaction was evident in combination with only the METCO 16C matrix. These reaction zones around the grit are shown in Figure 25. No reaction was exhibited with any of the other matrices in either the as-sprayed or aged condition.

Aluminum oxide - This grit material retained its sharp angular shape in combination with all matrices. No reaction, in either the as-sprayed or aged condition, was evident with METCO 443, METCO 16C, METCO 43C, or TRIBALOY T-400 matrices. This grit material was not evaluated in combination with the TIPALOY matrix material.

Silicon nitride - These abrasive grits were of poor quality. They exhibited rounded features that would not provide good cutting action against the abradable and had a porous structure, see Figure 26. No reaction was evident between METCO 443 and TIPALOY matrices in the as-sprayed or aged condition. TIPALOY and METCO 443 were the only matrices in which silicon nitride abrasive grits were evaluated in this program.

Metal Matrices

METCO 16C - This material produces a "splat free" type morphology when plasma spray coated. As shown in Figure 11, it appears as a dense, almost continuous coating on the METCO 443 bond coat. Some reaction occurs between METCO 16C and silicon carbide grits after aging, see Figure 25. A small amount of radial microcracking was observed particularly as a result of aging, and it is suspected that shrinkage due to sintering is the cause.

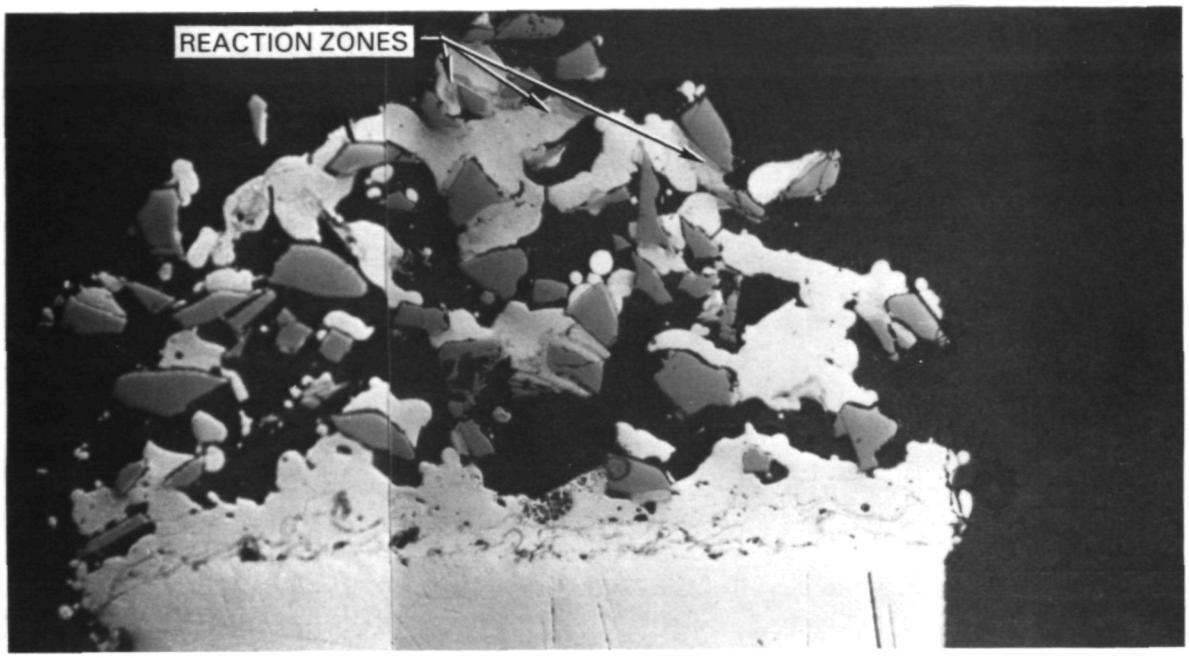

(100X)

Figure 25 Reaction of METCO 16C Matrix with Silicon Carbide (SiC) Grits.

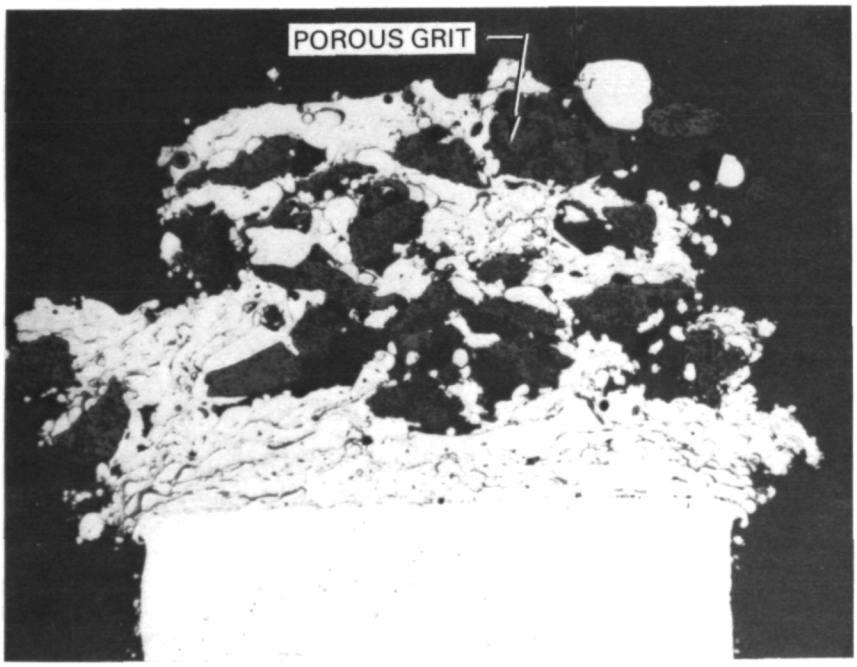

(100X)

Figure 26 Porous Structure and Rounded Features of Silicon Nitride (Si_3N_4) Grits.

METCO 443NS - The microstructure of the METCO 443 is a typical "splat type" which appears as layers between "stringers" of oxides that form on the melted particles as the coating is being built-up during successive passes of the spray gun, see Figures 14 and 15. Some cracking can be seen emanating from corners at the interface between the substrate and the bond coat. This cracking occurs in a random fashion, and is not peculiar to any specific coating or substrate material combination. METCO 443 was used as a 0.05-0.076 mm (0.002-0.003 inch) thick bond coat applied to all substrates prior to spraying with the candidate abrasive coatings.

METCO 43CNS - The METCO 43C exhibits the typical "splat" type microstructure, very similar to that of METCO 443, as is depicted in Figure 12 at high and low grit concentration levels. No microcracking is evident in the structure as the result of plasma spraying or aging.

TRIBALOY T-400 - This material produces a very dense "splat free" type microstructure when plasma sprayed as shown in Figure 16. A considerable amount of cracking is evident suggesting that the structure is highly stressed due to shrinkage upon solidification after the spray process.

TIPALOY - The microstructure of this material shows a typical "splat" type structure similar to METCO 443 after plasma-spraying. No microcracking is evident as a result of plasma spraying or aging. This material did not show any reaction with silicon carbide or silicon nitride abrasive grits. Silicon nitride grits were not evaluated in combination with a Tipaloy matrix in the program.

In summary, the results of the microscopic examinations show that:

1. TRIBALOY T-400 and METCO 16C are poor material choices for use as a matrix binder for abrasive grit systems due to microcracking of the coating structure and METCO 16C reacts with SiC grits.

2. The silicon nitride abrasive grits used in this study would not provide good coating rub performance due to the lack of edge sharpness and substantial grit porosity that would tend to weaken the grit structure.

3. As described under Section 3.2, Preparation of Specimens, coating porosity increases as grit concentration and grit size are increased due to "shadowing" that prevents filling of matrix material around the grit during the spray process.

3.3.2 Coating Adherence Tests

The mechanical testing was conducted per ASTM C633-69 at room temperature with a Tinius Olsen Universal Testing Machine shown in Figure 27. Adhesion specimens, "pull bars", of 25.4 mm (1.0 inch) in diameter were spray coated, on the circular ends, with the candidate abrasive coatings. A mating "pull bar" was bonded by an adhesive to the surface of the abrasive coating and

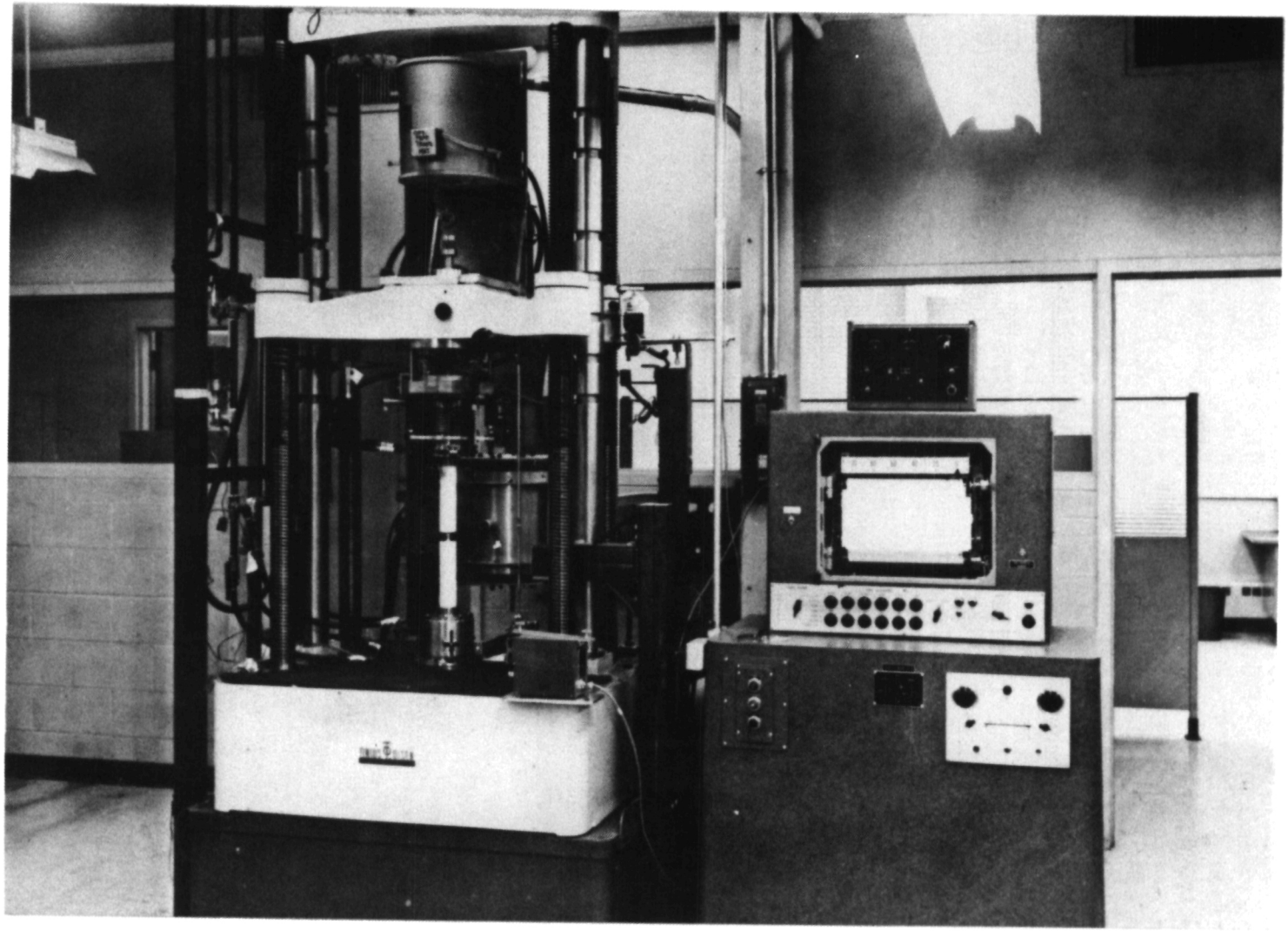

Figure 27 Tinus Olsen Universal Testing Machine.

tested using the tensile testing machine conforming to the requirements of ASTM methods E4, Verification of Testing Machines. To minimize the potential of penetration of the bonding adhesive into the thin 0.368 mm (0.015 inch) to 0.49 mm (0.020 inch) thick abrasive coating and masking the true test results, a special epoxy material, FM1000, purchased from American Cyanimide was utilized. This bonding material which comes in thin film sheet form is cut to size and is placed between the coating and the mating "pull bar". These mating pieces are then installed in a "Vee" block alignment fixture which applies a set spring load to the ends being joined. The loaded fixture is then installed in an oven for curing of the bond material for 1-1/2 hours at 436K (325°F) temperature. After curing of the adhesive, the specimen is tensile tested until failure of the coating or the adhesive has occurred. The adhesive has a tensile load capability of approximately 6895 N/cm^2 (10,000 lb/in^2) which is twice the tensile strength required for a typical plasma sprayed coating. The tensile strength of the coating is the load at failure divided by the cross sectional area of the coating.

Three bond adhesion tests were conducted for each abrasive tip treatment candidate to determine the average coating strength. Three tests gave, within practical limits, a higher degree of confidence in the results than by performing a single test and also allowed "weeding" out obvious erroneous results.

The results of these bond adhesion tests for the candidate abrasive coatings in the as-sprayed condition and aged for 100 hours at 866K (1100°F) temperature in air are shown in Table III. As can be seen in Table III, METCO 16C after being aged has the least bond strength of the matrix materials evaluated and does not meet the minimum bond strength, 3448 N/cm^2 (5000 lb/in^2), generally acceptable for plasma sprayed coatings; TRIBALOY T-400 coatings have poor bond strength in the as-sprayed condition, however, improve with aging. Due to the microcracking observed during microscopic examination, described in Section 3.3.1, a lower level of strength would be expected for both METCO 16C and TRIBALOY T-400. The adhesive strength capabilities of the coatings do not correlate well with grit concentration or grit size as may be expected. These variations are likely due to uncontrollable porosity variations, that weaken the coating structure, that occur during the spray process. The "shadowing" by the random depositing of single or multiple close packed grits, as they are sprayed with the matrix, results in incomplete and erratic filling of the matrix around the grits; thus, random voids exist in the coating.

The bond strength of coatings sprayed on nickel alloys is approximately 60 to 100 percent larger than coatings sprayed on titanium alloys. The strength of coatings on the nickel alloy substrates in the majority of the cases, except for coatings with large grits, exceeded the epoxy adhesive strength; the failure occurred in the adhesive rather than the coating. The coatings on titanium substrates failed either within the coating or at the coating-to-substrate interface. A weaker bond would be expected on titanium substrates since considerably more oxidation takes place at the interface between the METCO 443 bond coat and the titanium than at the interface between the METCO 443 and nickel during the spray process, see Figure 28.

TABLE III

ADHESIVE STRENGTH TEST RESULTS

Test Phase	Matrix Material	Grit Material	Grit Size No.	Substrate Material	Grit Conc. Average %	As-Sprayed Coating Strength $N/cm^2 x 10^{-3}$ (ksi)	Aged Coating Strength $N/cm^2 x 10^{-3}$ (ksi)
1	Metco 443	SiC	150	Ti-6Al-4V	42	4.50 (6.53)	2.89 (4.20)
1	Metco 443	SiC	150	Ti-6Al-4V	17	2.62 (3.80)	4.61 (6.69)
1	Metco 443	Al_2O_3	150	Ti-6Al-4V	40	4.57 (6.63)	5.64 (8.18)
1	Metco 443	Al_2O_3	150	Ti-6Al-4V	25	4.25 (6.16)	5.37 (7.79)
1	Metco 43C	SiC	150	Ti-6Al-4V	37	4.19 (6.08)	5.00 (7.25)
1	Metco 43C	SiC	150	Ti-6Al-4V	16	4.45 (6.45)	3.25 (4.71)
1	Metco 43C	Al_2O_3	150	Ti-6Al-4V	23	4.89 (7.09)	2.73 (3.96)
1	Metco 43C	Al_2O_3	150	Ti-6Al-4V	30	3.75 (5.44)	5.91 (8.57)
1	Metco 16C	SiC	150	Ti-6Al-4V	38	2.16 (3.13)	1.92 (2.79)
1	Metco 16C	SiC	150	Ti-6Al-4V	18	2.30 (3.33)	1.77 (2.56)
1	Metco 16C	Al_2O_3	150	Ti-6Al-4V	47	3.76 (5.46)	1.78 (2.58)
1	Metco 16C	Al_2O_3	150	Ti-6Al-4V	31	3.61 (5.23)	1.38 (2.02)
1	Tribaloy 400	SiC	150	Ti-6Al-4V	37	1.88 (2.72)	4.09 (5.93)
1	Tribaloy 400	SiC	150	Ti-6Al-4V	26	2.08 (3.01)	4.81 (6.97)
1	Tribaloy 400	Al_2O_3	150	Ti-6Al-4V	39	1.94 (2.82)	3.84 (5.57)
1	Tribaloy 400	Al_2O_3	150	Ti-6Al-4V	6	2.18 (3.16)	3.61 (5.23)
3	Metco 443	SiC	150	Inconel 718	25	8.27 (12)	7.79 (11.3)
3	Metco 443	SiC	150	Inconel 718	23	8.96 (10.1)	7.58 (11.0)
3	Metco 443	Si_3N_4	150	Inconel 718	39	7.86 (11.4)	6.55 (9.5)
3	Metco 443	Si_3N_4	150	Inconel 718	22	6.62 (9.6)	6.41 (9.3)
3	Tipaloy	SiC	150	Inconel 718	35	6.14 (8.9)	7.86 (11.4)
3	Tipaloy	SiC	150	Inconel 718	20	4.34 (6.3)	8.07 (11.7)
3	Tipaloy	Si_3N_4	150	Inconel 718	30	8.0 (11.6)	7.93 (11.5)
3	Tipaloy	Si_3N_4	150	Inconel 718	12	6.83 (9.9)	7.24 (10.5)
3	Metco 443	SiC	54	Inconel 718	--	3.93 (5.7)	6.83 (9.9)
3	Tipaloy	SiC	54	Inconel 718	--	4.91 (7.12)	6.89 (10.0)
3	Tipaloy	SiC	54	Inconel 718	--	1.65 (2.40)	2.48 (3.60)
3	Tipaloy	Si_3N_4	150	Inconel 718	--	3.59 (5.20)	3.79 (5.50)

Coatings with large No. 54 abrasive grits exhibit somewhat lower and erratic strength levels than coatings with smaller No. 150 grits, see Table III. This can be attributed to substantial variations in the coating porosity, inherent to large grits, that occurs during the spray process, see Section 3.2.

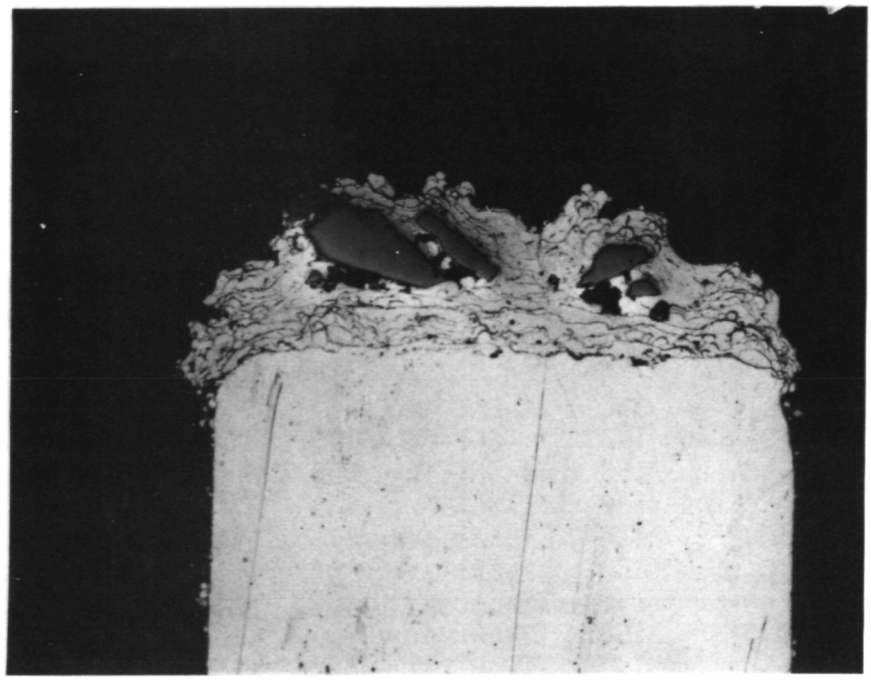

(100X)

NICKEL ALLOY SUBSTRATE

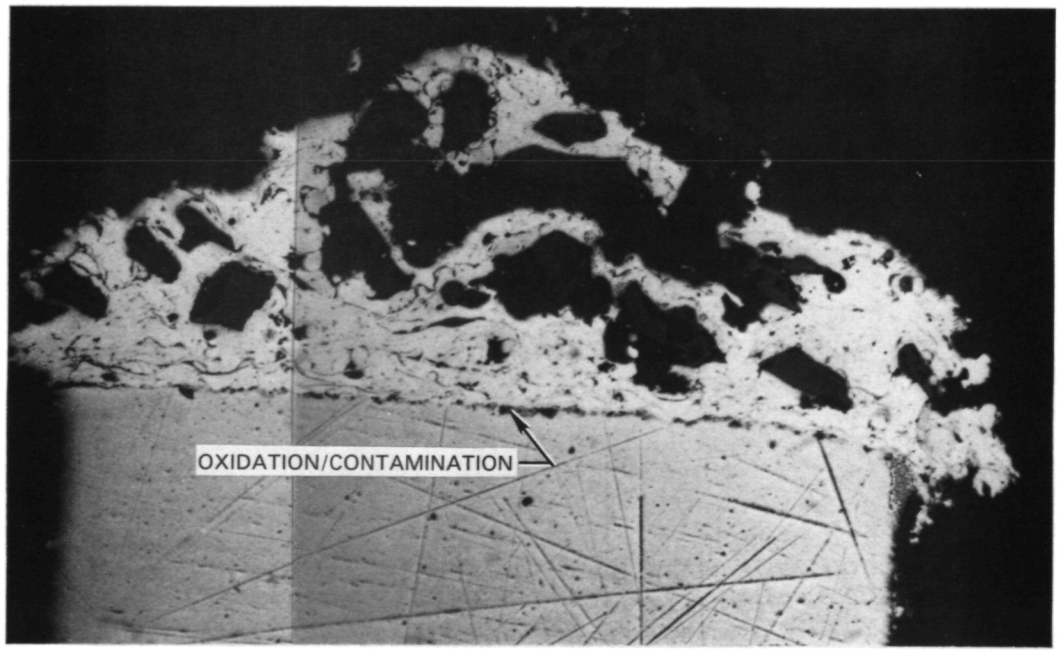

(100X)

TITANIUM ALLOY SUBSTRATE

Figure 28 Microphotograph of Oxidation/Contamination at Coating-to-Substrate Interface for Titanium and Nickel Based Alloy Substrates.

3.3.3 Erosion Testing

To determine the relative erosion resistance of the various candidate abrasive coating systems, erosion tests were conducted in the rig shown in Figure 29. This rig incorporates a long tube to accelerate the particulate up to gas velocity at the discharge end. A precalibrated power feeder dispenses the particulate at the required feed rate into a nitrogen carrier gas stream which delivers the particulate to the rig just upstream of the acceleration tube. The particulate velocity at the acceleration tube discharge is set in accordance with a precalibration of the rig flow system based on Laser Doppler Velocimeter measurements. The particulate impingement angle is set by rotation adjustments incorporated into the specimen mount.

Each candidate abrasive coating was erosion tested using consistent rig conditions to ensure results that can be compared directly. These test conditions are as follows:

Particle velocity - 320 meters/second (1050 feet/second)
Impingement angle - 15 degrees
Temperature - room
Particulate - No. 240 Al_2O_3 grit

A test procedure was established to ensure that a consistent method was used for each test. The rig systems were checked for proper operation, and the powder feeder reservoir was filled with a weighed amount of particulate. The impingement angle was set and the coating specimen to be erosion tested was carefully weighted and installed in the rig. The air supply pressure regulating valve was slowly opened to establish the rig pressure levels, as dictated by the precalibration, required to produce the desired particle velocity. The particle feeder was then turned on to initiate the erosion test and was turned off after one minute to terminate the test. After the test, the specimen and the particulate were weighed. By subtraction of the post-test from the pretest weight measurements, the amount of specimen material eroded away and the amount of particulate used during the test was determined. The data were reduced in terms of erosion mass parameter (grams of coating material eroded per gram of abrasive impacted on the specimen) and the results determined are shown on Table IV; also shown for comparison is the erosion parameters measured for uncoated titanium, nickel, and iron based alloys typically used for compressor blades.

A comparison of these erosion results show that all the candidate coatings have less erosion resistance than uncoated blade material alloys. In general, erosion resistance is improved by aging for 100 hours at 866K (1100°F) temperature in air. The erosion of TRIBALOY and METCO 16C matrix coatings is considerably higher than any of the other candidate matrix materials evaluated. This lower erosion resistance is more than likely associated with the microcracked (thus, weaker) structure of these two materials as described in Section 3.3.1, Microscopic Examinations. The erosion of the coatings does not appear to be particularly sensitive to the grit material or grit size used in combination with any of the matrix materials. Also, the substrate material (titanium, nickel, or iron based alloys) on which METCO 443 abrasive coatings were sprayed did not significantly influence the coating erosion resistance.

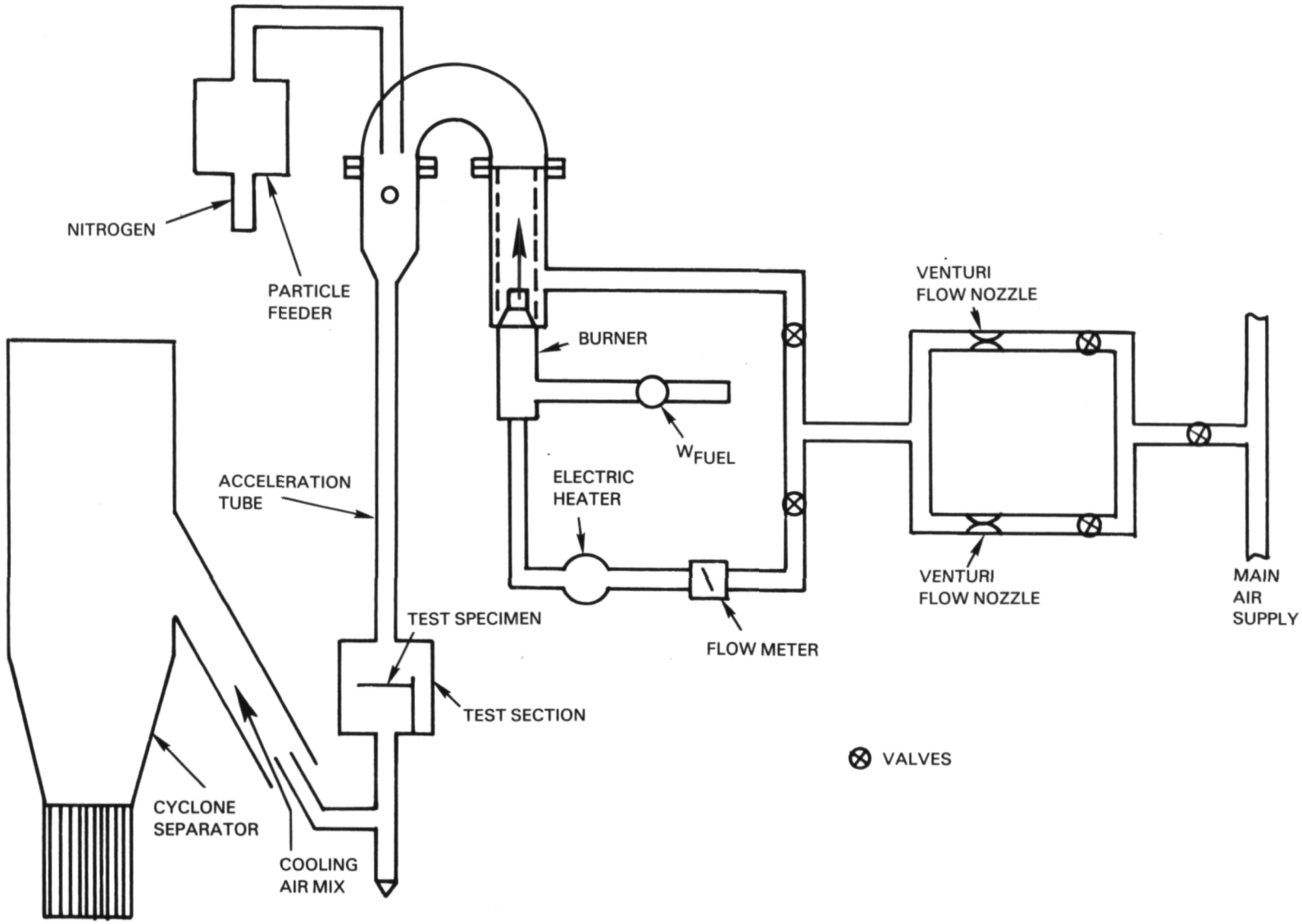

Figure 29 Schematic of Erosion Test Facility.

TABLE IV

EROSION TEST RESULTS

Test Phase	Matrix Material	Grit Material	Grit Size No.	Substrate Material	Grit Conc. Average %	As-Sprayed Erosion Parameter Gm. Removed Gm. Particulate	Aged Erosion Parameter Gm. Removed Gm. Particulate
1	Metco 443	SiC	150	Ti-6Al-4V	42	0.017	0.012
1	Metco 443	Sic	150	Ti-6Al-4V	17	0.021	0.011
1	Metco 443	Al_2O_3	150	Ti-6Al-4V	40	0.017	0.012
1	Metco 443	Al_2O_3	150	Ti-6Al-4V	25	0.016	0.014
1	Metco 43C	SiC	150	Ti-6Al-4V	37	0.017	0.014
1	Metco 43C	SiC	150	Ti-6Al-4V	16	0.016	0.014
1	Metco 43C	Al_2O_3	150	Ti-6Al-4V	23	0.016	0.019
1	Metco 43C	Al_2O_3	150	Ti-6Al-4V	30	0.016	0.017
1	Metco 16C	SiC	150	Ti-6Al-4V	38	0.04	0.022
1	Metco 16C	SiC	150	Ti-6Al-4V	18	0.047	0.023
1	Metco 16C	Al_2O_3	150	Ti-6Al-4V	47	0.039	0.027
1	Metco 16C	Al_2O_3	150	Ti-6Al-4V	31	0.044	0.028
1	Tribaloy 400	SiC	150	Ti-6Al-4V	37	0.155	0.036
1	Tribaloy 400	SiC	150	Ti-6Al-4V	26	0.086	0.033
1	Tribaloy 400	Al_2O_3	150	Ti-6Al-4V	39	0.122	0.035
1	Tribaloy 400	Al_2O_3	150	Ti-6Al-4V	6	0.138	0.034
2	Metco 443	SiC	90	Greek Ascoloy	32	0.010	0.014
2	Metco 443	SiC	90	Greek Ascoloy	9	0.013	0.012
2	Metco 443	SiC	90	Inconel 718	32	0.013	0.015
2	Metco 443	SiC	90	Inconel 718	9	0.011	0.013
2	Metco 443	SiC	90	Ti-6Al-4V	32	0.012	0.013
2	Metco 443	SiC	90	Ti-6Al-4V	9	0.014	0.013
3	Metco 443	SiC	150	Inconel 718	25	0.037	0.018
3	Metco 443	SiC	150	Inconel 718	23	0.015	0.013
3	Metco 443	Si_3N_4	150	Inconel 718	39	0.015	0.012
3	Metco 443	Si_3N_4	150	Inconel 718	22	0.016	0.013
3	Tipaloy	SiC	150	Inconel 718	35	0.041	0.025
3	Tipaloy	SiC	150	Inconel 718	20	0.018	0.017
3	Tipaloy	Si_3N_4	150	Inconel 718	30	0.012	0.013
3	Tipaloy	Si_3N_4	150	Inconel 718	12	0.014	0.014
3	Metco 443	SiC	54	Inconel 718	--	0.018	0.018
3	Tipaloy	SiC	54	Inconel 718	--	0.024	0.019
3	Tipaloy	SiC	54	Inconel 718	--	0.016	0.013
3	Tipaloy	Si_3N_4	54	Inconel 718	--	0.012	0.017
	Uncoated	--	--	Greek Ascoloy	--	0.0055	--
	Uncoated	--	--	Inconel 718	--	0.0052	--
	Uncoated	--	--	Ti-6Al-4V	--	0.005	--

3.3.4 Rub Testing

The object of the rub tests was to determine the effectiveness of each candidate blade abrasive tip treatment for removing seal abradable material under simulated engine rub conditions. The basic measure of rub effectiveness used was volume wear ratio (VWR), which is the volume of abradable seal material removed divided by the volume of blade tip abrasive material removed during the rub test.

The rub tests were conducted on a small scale abradability rig as shown in Figure 30; a schematic of the rig is shown in Figure 31. This rig utilizes an 203.0 mm (8.0 inch) diameter rotor with dovetail slots for mounting the coated tip specimens and is driven by an air turbine with a governor to control speed. The stationary abradable rub shoe is mounted on a carriage which is supported on two rails by low friction bearings and is driven toward the rotating blades by a pulley and weight system. Controlled interaction rates are achieved with a variable motor micrometer feed system which acts to restrain the motion of the carriage against the weight system. To measure carriage travel, an instrumentation system, which utilizes a linear velocity displacement transformer (LVDT), whose output voltage is calibrated against carriage distance, was used. To measure normal and tangential forces, a piezoelectric load cell manufactured by Kistler Corporation was mounted between the rub shoe and carriage.

The rub shoe abradable was a plasma-sprayed porous nichrome deposited on 1.27-mm (0.05-inch) thick, 50.8-mm (2-inch) wide stainless steel substrates that had a radius of curvature slightly larger than the blade tip radius, 108 mm (4.25 inches); the rub length was over a 60-degree arc. The abradable material was plasma-sprayed at a higher density hence higher hardness, than normally used for advanced engine compressor gas-path seals. This higher density abradable was selected to ensure a surface with sufficient rub resistance to adequately "work" the abrasive coatings during the rub tests.

All rub tests were conducted at 335 m/sec (1100 ft/sec) blade tip velocity, 0.0254 mm/sec (0.001 inch/sec) interaction rate for a total rub interaction of 1.27 mm (0.050 inch). This tip velocity is representative of compressor blade tip speeds at high power engine conditions and the interaction rate and incursion depth reflect transient thermal closures between the case and rotor during engine acceleration between idle and take-off power. Since coating wear is dependent on the test conditions imposed, trial rub tests were conducted to ensure that the conditions selected were severe enough to induce adequate wear to properly evaluate the rub effectiveness of the various candidate coatings.

The rub tests were conducted using a consistent approach for each candidate tip treatment evaluated. The coated blades were initially measured for length. The blades were then installed in the rotor, the rotor balanced and installed in the abradability rig. The start of the interaction depth (zero point) was established by moving the abradable rub shoe/carriage assembly until the shoe just touched the blade. A limit switch, which is activated by the LVDT, is set to cut off power to the carriage microfeed drive motor when the interaction depth of 1.27 mm (0.05 inch) is reached. At the end of the test, a pneumatic piston is activated to retract the carriage.

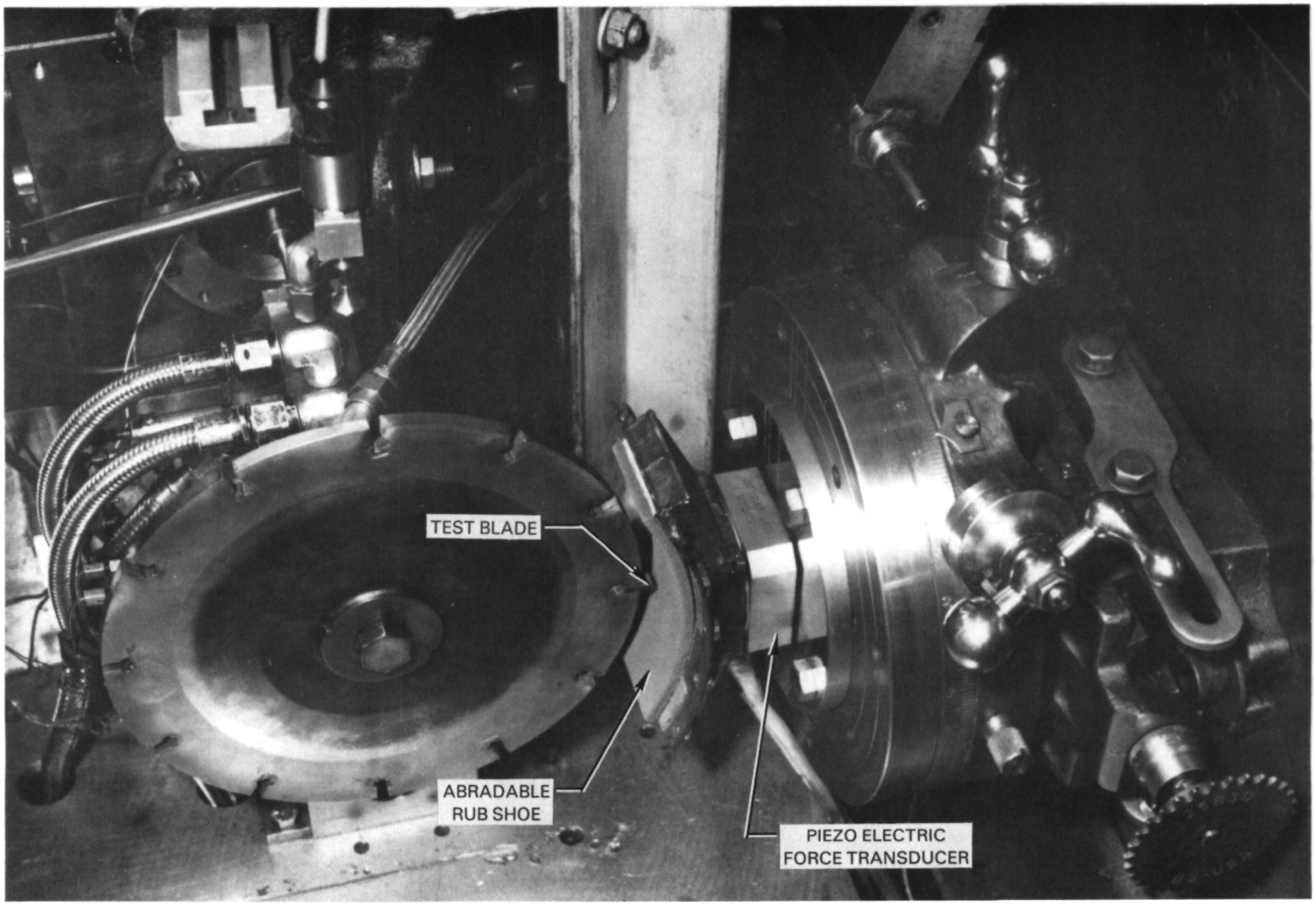

Figure 30 Rig for Conducting Rub Tests.

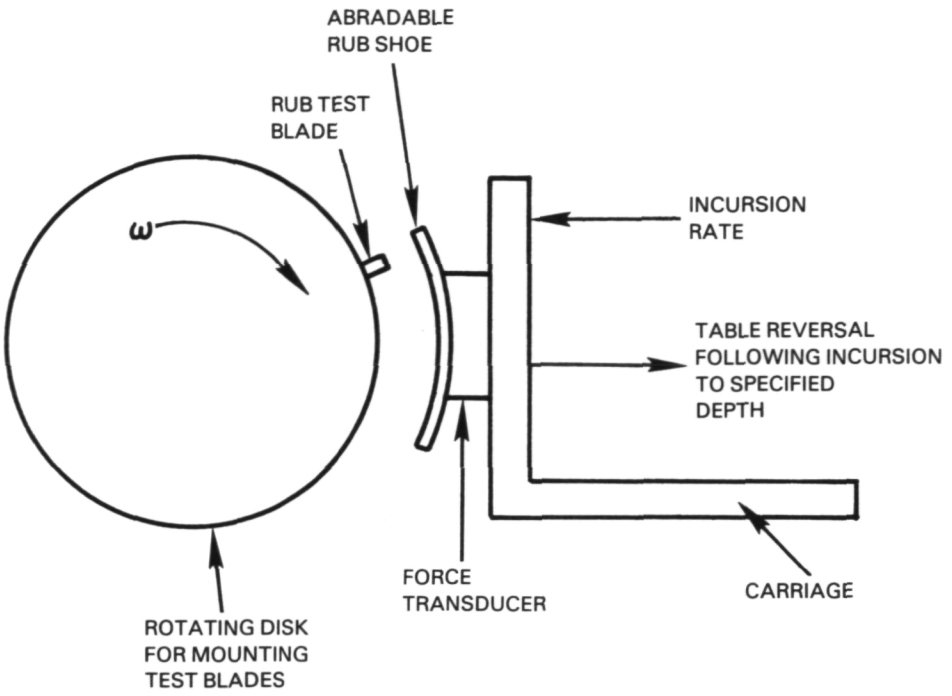

Figure 31 Schematic of Rub Test Rig.

Prior to each test, the rub shoe was translated to the side, away from the rotating blade, using a lathe turret type adjustment feature and a pretest check was conducted. The interaction depth and instrumentation settings were checked including the systems to operate the rig. The rub shoe was returned to the operating position while monitoring the rig bearing system for temperature and vibration. The test was then conducted following a set procedure and ended when the carriage interaction was stopped by the limit switch and the carriage was withdrawn by the pneumatic piston.

During the tests, tangential and normal forces were measured. The piezoelectric force transducer signals were fed to amplifier and conditioning circuitry which provided continuous recording of the force data on magnetic tape and later played back for analysis. The frequency response sensitivity range and load capacity of the force transducers selected was 0 to 5000 Hertz and 0 to 8896N (2000 pounds) which was well within the 430 Hertz and 0 to 88.96N (20 pounds) maximum force range expected for the single blade rub tests.

Subsequent play back of the force data encountered difficulties primarily with the masking of the real forces by extraneous forces induced by frequencies inherent to the rig. Attempts to filter out the extraneous frequencies in a systematic fashion, all the way down to the blade passing frequency, were not successful. A series of static diagnostic tests indicated significant flexing of the rub shoe at the ends and vibratory motion about the shoe/load-cell/carriage-mount system. Shortening the shoe in an effort to reduce the end flexing and stiffening the shoe holder mount, did not noticeably improve the

system. Excitation of the entire rub shoe and mount system occurred as the blade entered and exited the rub shoe. This excitation induced extraneous vibration levels at the load cell which resulted in erroneous output measurements. Consultation with P&W instrumentation and vibration experts resulted in a conclusion that the problem was very complex and that a reliable solution to the problem with the existing rig design was beyond the scope of the program; the rub evaluation was then focused on the wear results.

As stated previously, the measure of rub effectiveness used to evaluate the abrasive coatings in this program is volume wear ratio (VWR), the volume of seal material removed divided by the volume of tip abrasive material removed from the blade. To determine the volume of tip material removed, the blade length was measured prior to and after the rub test and the difference in these two measurements was multiplied by the coating cross section normal to the blade tip. To determine the average wear in cases where the blade wear was significantly irregular, a shadowgraph technique was used that involved enlargement the rub surface to 10X and applying "Simpsons Rule" of areas over the width of the blade. To determine the volume of the abradable seal material removed during the rub, a series of careful measurements were made to determine the average rub groove profile (width and depth) over the groove chord length. These key dimensions, along the rub shoe radius of curvature, were then input to a computer which was specifically programmed to calculate the groove volume. The resulting volume wear ratios and all major rub data for the various candidate matrix/abrasive grit coatings tested, and comparative uncoated titanium, nickel, and iron based alloy blade rub results, are listed in Table V. Comparing the key volume wear ratio results indicate in general that:

1. Abrasive tip treatment improves the rub performance of uncoated blades.

2. Aluminum oxide and silicon nitride grits generally do not perform as well as silicon carbide grits with the exception of aluminum oxide grits in METCO 16C matrices.

3. Abrasive coatings with TRIBALOY T-400 and TIPALOY matrices show inferior rub capabilities.

4. Aging appears to improve rub effectiveness for the majority of coating combinations.

5. Coatings with grits larger than No. 150 do not improve rub performance.

TABLE V

RUB TEST RESULTS

Test Phase	Substrate Material	Matrix Material	Grit Material	Grit Size No.	Grit Conc. Average (%)	As Sprayed			Aged		
						Blade Wear mm (in)	Abradable Groove Avg. Depth mm (in)	Volume Wear Ratio	Blade Wear mm (in)	Abradable Groove Avg. Depth mm (in)	Volume Wear Ratio
1	Ti-6Al-4V	Metco 443	SiC	150	42	0.424 (0.0167)	0.610 (0.024)	192	0.292 (0.0115)	0.279 (0.011)	98
1	Ti-6Al-4V	Metco 443	SiC	150	17	0.805 (0.0317)	0.305 (0.012)	42	0.114 (0.0045)	1.09 (0.043)	1238
1	Ti-6Al-4V	Metco 443	Al_2O_3	150	40	0.551 (0.0217)	0.457 (0.018)	98	0.673 (0.0265)	0.559 (0.022)	95
1	Ti-6Al-4V	Metco 443	Al_2O_3	150	25	0.310 (0.0112)	0.838 (0.033)	382	0.208 (0.0082)	0.940 (0.037)	585
1	Ti-6Al-4V	Metco 43C	SiC	150	37	0.864 (0.034)	0.152 (0.006)	13	0.381 (0.015)	0.533 (0.021)	182
1	Ti-6Al-4V	Metco 43C	SiC	150	16	0.305 (0.012)	0.838 (0.033)	356	0.076 (0.003)	0.889 (0.035)	1556
1	Ti-6Al-4V	Metco 43C	Al_2O_3	150	23	0.533 (0.021)	0.533 (0.021)	88	0.475 (0.0187)	0.330 (0.013)	81
1	Ti-6Al-4V	Metco 43C	Al_2O_3	150	30	0.686 (0.027)	0.559 (0.022)	55	0.284 (0.0112)	0.533 (0.021)	256
1	Ti-6Al-4V	Metco 16C	SiC	150	38	0.787 (0.031)	0.279 (0.011)	33	0.589 (0.0232)	0.432 (0.017)	87
1	Ti-6Al-4V	Metco 16C	SiC	150	18	0.557 (0.022)	0.457 (0.018)	112	0.170 (0.0067)	0.965 (0.038)	711
1	Ti-6Al-4V	Metco 16C	Al_2O_3	150	47	0.127 (0.005)	1.244 (0.049)	1548	0.069 (0.0027)	1.016 (0.040)	1716
1	Ti-6Al-4V	Metco 16C	Al_2O_3	150	31	0.953 (0.0375)	0.432 (0.017)	43	0.069 (0.0027)	1.016 (0.040)	1848
1	Ti-6Al-4V	Tribaloy T-400	SiC	150	37	0.559 (0.022)	0.432 (0.017)	58	0.526 (0.0207)	0.330 (0.013)	68
1	Ti-6Al-4V	Tribaloy T-400	SiC	150	26	0.381 (0.015)	0.787 (0.031)	243	0.368 (0.0145)	0.508 (0.020)	183
1	Ti-6Al-4V	Tribaloy T-400	Al_2O_3	150	39	0.381 (0.037)	0.305 (0.012)	23	0.495 (0.0195)	0.483 (0.019)	135
1	Ti-6Al-4V	Tribaloy T-400	Al_2O_3	150	6	0.864 (0.034)	0.203 (0.008)	16	0.737 (0.029)	0.229 (0.009)	31
2	Greek Ascoloy	Metco 443	SiC	90	32	1.09 (0.043)	0.127 (0.005)	4	0.864 (0.034)	0.305 (0.012)	24
2	Greek Ascoloy	Metco 443	SiC	90	9	0.432 (0.017)	0.762 (0.030)	286	0.686 (0.027)	0.610 (0.024)	128
2	Inconel 718	Metco 443	SiC	90	32	0.356 (0.014)	0.838 (0.033)	405	0.356 (0.014)	0.381 (0.015)	92
2	Inconel 718	Metco 443	SiC	90	9	0.610 (0.024)	0.533 (0.021)	126	0.254 (0.010)	0.813 (0.032)	367
2	Ti-6Al-4V	Metco 443	SiC	90	32	1.143 (0.045)	0.102 (0.004)	7	0.356 (0.014)	1.04 (0.041)	368
2	Ti-6Al-4V	Metco 443	SiC	90	9	0.559 (0.022)	0.660 (0.026)	184	0.813 (0.032)	0.787 (0.031)	105
3	Inconel 718	Metco 443	SiC	150	25	0.508 (0.020)	0.686 (0.027)	280	0.127 (0.005)	1.09 (0.043)	1298
3	Inconel 718	Metco 443	SiC	150	23	0.229 (0.009)	1.04 (0.041)	451	0.373 (0.0147)	0.889 (0.035)	194
3	Inconel 718	Metco 443	Si_3N_4	150	39	0.508 (0.020)	0.711 (0.028)	246	0.508 (0.020)	0.686 (0.027)	157
3	Inconel 718	Metco 443	Si_3N_4	150	22	0.432 (0.017)	0.864 (0.034)	246	0.533 (0.533)	0.787 (0.031)	187
3	Inconel 718	Tipaloy	SiC	150	35	0.381 (0.015)	0.762 (0.030)	231	0.229 (0.009)	1.016 (0.040)	510
3	Inconel 718	Tipaloy	SiC	150	20	0.229 (0.009)	0.991 (0.039)	384	1.09 (0.043)	0.076 (0.003)	4
3	Inconel 718	Tipaloy	Si_3N_4	150	30	0.864 (0.034)	0.406 (0.016)	46	1.09 (0.043)	0.203 (0.008)	26
3	Inconel 718	Tipaloy	Si_3N_4	150	12	0.762 (0.030)	0.457 (0.018)	39	0.533 (0.021)	0.610 (0.024)	124
3	Inconel 718	Metco 443	SiC	54	--	0.508 (0.020)	0.584 (0.023)	130	0.711 (0.028)	0.660 (0.026)	101
3	Inconel 718	Tipaloy	SiC	54	--	0.381 (0.015)	0.711 (0.028)	198	0.279 (0.011)	0.711 (0.028)	343
3	Inconel 718	Tipaloy	SiC	54	--	0.203 (0.008)	0.889 (0.035)	639	0.178 (0.007)	0.965 (0.038)	612
3	Inconel 718	Tipaloy	Si_3N_4	54	--	0.737 (0.029)	0.432 (0.017)	53	0.559 (0.522)	0.406 (0.016)	74
	Greek Ascoloy	Uncoated	--		--	0.787 (0.037)	0.508 (0.020)	120			
	Inconel 718	Uncoated	--		--	0.737 (0.029)	0.508 (0.020)	110			
	Ti-6Al-4V	Uncoated	--		--	0.686 (0.027)	0.305 (0.012)	19			

Observations of post-test abradable shoe and coated blade hardware show clearly that the coatings with high rub effectiveness groove deeper into the abradable and exhibit less blade coating removal than coatings with low rub effectiveness. Typical blade wear and corresponding abradable shoe wear patterns for the abrasive coatings tested are illustrated in Figures 32 and 33, respectively. The uneven wear on the rub shoe on the left in Figure 33, i.e. lack of wear in the center portion, was caused by the interactive rub between the rotating blade and the stationary rub shoe where the blade radius was larger than the radius of curvature of the rub shoe. This mismatch in radii is due to the adverse dimensional build up of tolerances during fabrication of the plasma-sprayed abradable shoe and the abrasive coated blade; this mismatch occured for only a limited number of tests (10%). This uneven wear is not expected significantly affect the test results since the the eneven wear should not influence the material properties or the frictional characteristics which are the primary factors that govern blade or shoe wear. In comparison, the rather shallow wear grooves in the abradable shown in Figure 34 were rubbed with the uncoated titanium, nickel, and iron based alloy blades shown in Figure 35.

3.4 DATA EVALUATION AND ANALYSIS

The evaluation of the candidate coating systems was based on the results of microscopic examinations and rub, erosion, and bond adherence tests conducted on the coatings as described in Section 3.3. The effects of aging for 100 hours at 866K (1100°F) in air on coating performance was also assessed. This evaluation was performed, consistent with the requirements of the program, in three Phases.

3.4.1 Phase 1 - Screening Tests

This phase of the test evaluation was to conduct screening tests to select the best matrix/abrasive coating combination from four matrix materials (METCO 16C, METCO 43C, METCO 443, and TRIBALOY T-400) and two abrasive grit materials (silicon carbide and aluminum oxide). The coatings were plasma-sprayed on titanium based alloy test specimens with No. 150 size grits at two grit concentration levels.

Summarized below are the results of the evaluation that established silicon carbide abrasive grits in combination with a METCO 443 matrix as the better abrasive coating choice of the candidate matrix/abrasive materials tested:

Microscopic Examinations:

1. METCO 16C and TRIBALOY T-400 matrix materials produced microcracking in the coating that would tend to weaken the structure. METCO 16C also reacts with silicon carbide grits during the aging process.

2. METCO 443 and METCO 43C matrices have similar coating structures with no microcracking or reaction with silicon carbide or aluminum oxide grits.

3. Coatings with high grit concentration result in higher coating porosity than coatings with low grit concentration.

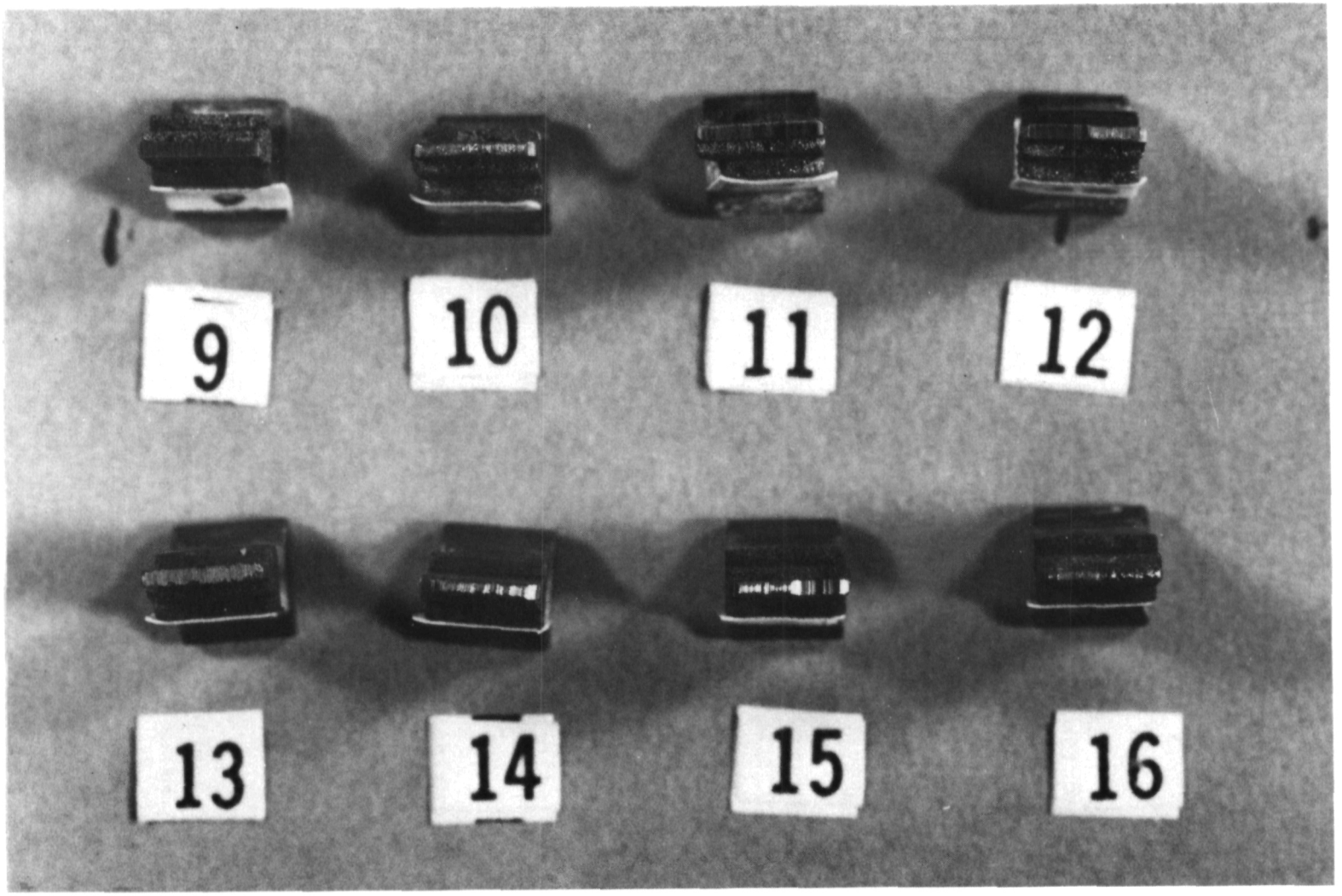

3X

BLADE ABRASIVE MATERIALS USING NO. 150 GRIT

NO.	MATRIX	GRIT	CONC.	COND.	NO.	MATRIX	GRIT	CONC.	COND.
9	METCO 43C	SiC	37%	AS SPRAYED	13	METCO 443	SiC	42%	AGED
10	METCO 43C	Al_2O_3	30%	AS SPRAYED	14	METCO 443	SiC	17%	AGED
11	TRIBALOY	Al_2O_3	6%	AS SPRAYED	15	METCO 443	Al_2O_3	40%	AGED
12	TRIBALOY	SiC	37%	AS SPRAYED	16	METCO 443	Al_2O_3	25%	AGED

Figure 32 Typical Abrasive Blade Tips after Rubbing Against Abradable (shown in Figure 33).

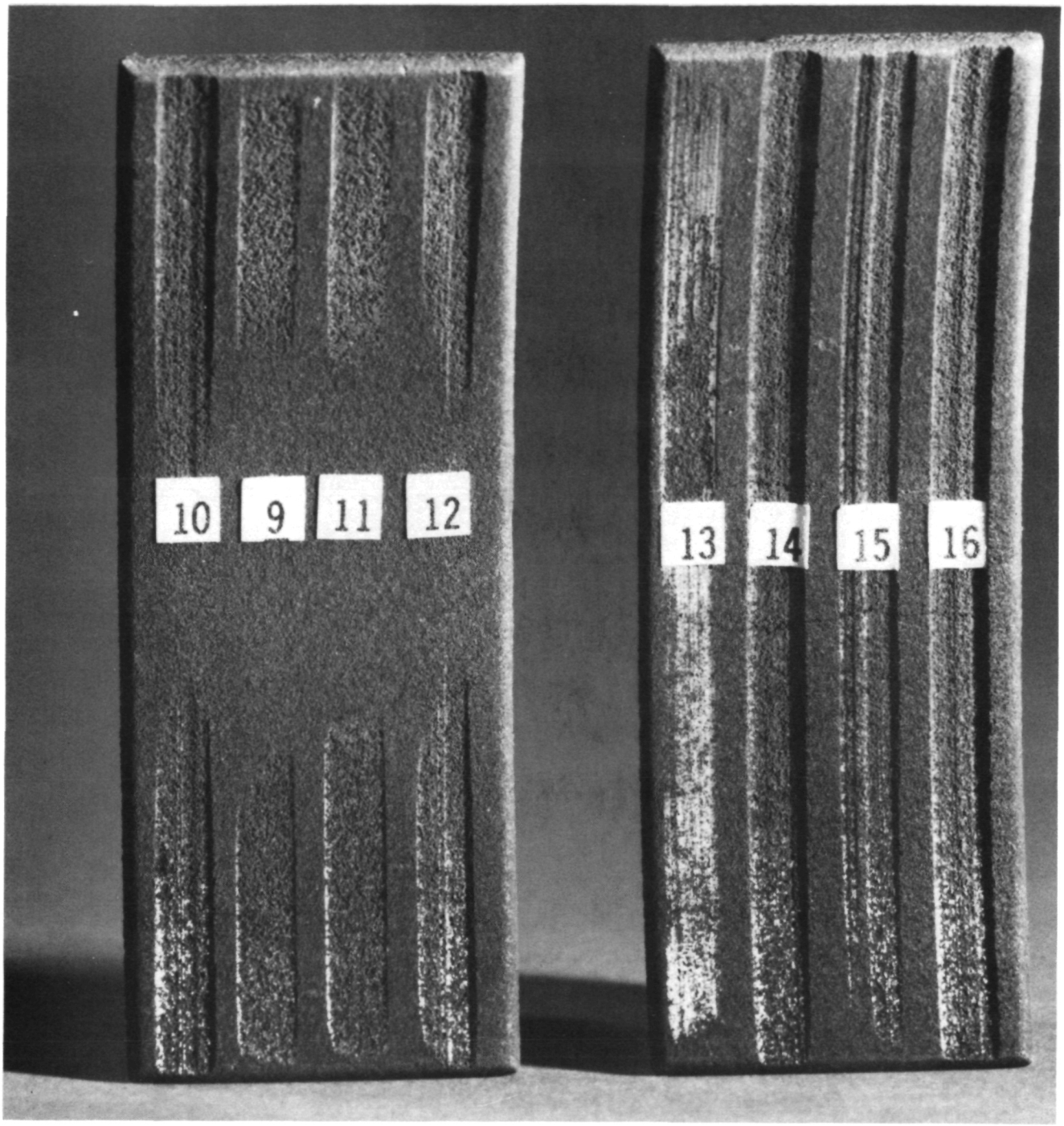

1.5X

BLADE ABRASIVE MATERIALS USING NO. 150 GRIT

NO.	MATRIX	GRIT	CONC.	COND.	NO.	MATRIX	GRIT	CONC.	COND.
9	METCO 43C	SiC	37%	AS SPRAYED	13	METCO 443	SiC	42%	AGED
10	METCO 43C	Al_2O_3	30%	AS SPRAYED	14	METCO 443	SiC	17%	AGED
11	TRIBALOY	Al_2O_3	6%	AS SPRAYED	15	METCO 443	Al_2O_3	40%	AGED
12	TRIBALOY	SiC	37%	AS SPRAYED	16	METCO 443	Al_2O_3	25%	AGED

Figure 33 Typical Abradable Shoe Rub Grooves Resulting from Rubs by Abrasive Tip Coatings (shown in Figure 32).

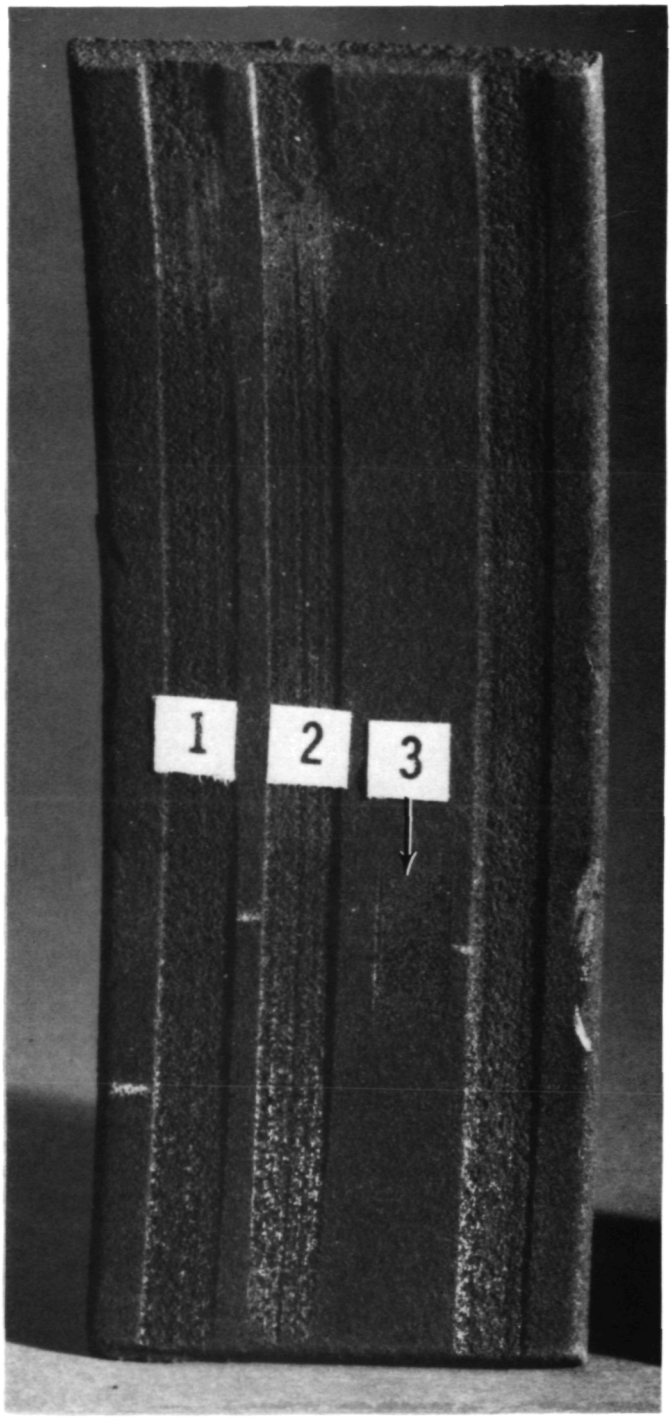

UNCOATED BLADE MATERIALS 1.5X

NO.
1 GREEK ASCOLOY
2 INCONEL 718
3 Ti-6Al-4V

Figure 34 Typical Abradable Shoe Rub Grooves Resulting from Rubs by Uncoated Blades (shown in Figure 35).

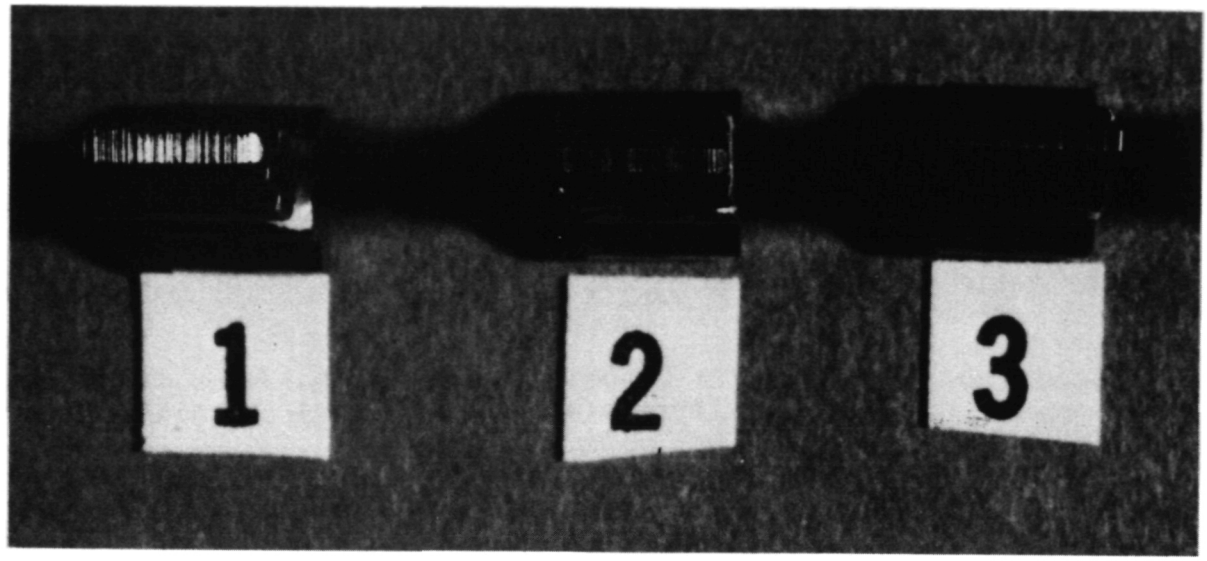

3X

UNCOATED BLADE MATERIALS

NO.	
1	GREEK ASCOLOY
2	INCONEL 718
3	Ti-6Al-4V

Figure 35 Uncoated Blades after Rubbing Against Abradable (shown in Figure 34).

Adherence Testing:

1. METCO 16C matrix coatings result in significantly lower bond strengths than the other coating matrices evaluated and, after aging, does not meet the minimum bond strength, 3448 N/cm^2 (5000 psi) generally acceptable for plasma-sprayed coatings.

2. TRIBALOY T-400 matrix coatings have poor bond strengths in the as-sprayed condition, though aging significantly improved the bond strength by a factor of two.

Erosion Testing:

1. TRIBALOY T-400 matrices have significantly higher erosion levels, particularly in the as-sprayed condition, than the other candidate matrix materials evaluated.

2. METCO 443 and METCO 43C matrices have much better erosion resistance when compared to METCO 16C and TRIBALOY T-400.

Rub Testing:

1. In general, coating matrices comprised of silicon carbide grits result in much better rub performance than coatings with aluminum oxide grits, except when in combination with METCO 16C matrices.

2. METCO 16C in combination with aluminum oxide grits has better wear resistance, than when in combination with silicon carbide grits.

3. Coatings with TRIBALOY T-400 matrices performed poorly in rub evaluations; volume wear ratios are 1/4 to 1/6 of that demonstrated by the other candidate abrasive coating systems.

4. Coatings with low grit concentrations (15 to 30 percent) have, in general, substantially better wear resistance than coatings with high grit concentrations (30 to 50 percent).

Erosion and adhesion test results did not show a dependency on grit concentration level. Based on the rub test results, however, lower grit concentrations in the 15 to 30 percent range would be the better selection.

Based on this overall evaluation, METCO 443 or METCO 43C in combination with silicon carbide grits plasma-sprayed at a 15 to 20 percent grit concentration level would provide equally good performance as an abrasive tip treatment on compressor blades. METCO 443, however, was selected as the better matrix because of its good qualities as a universal bond coat, and it can be applied as a "single layer" plasma-sprayed system at reduced coat.

3.4.2 Phase 2 - Further Development of Matrix/Abrasive Coating

This phase of the program was directed toward further development of the matrix/abrasive coating material combination selected in Phase 1. The selected METCO 443 matrix and silicon carbide grit coating was test evaluated on titanium, nickel, and iron based alloy substrates (Ti-6Al-4V, Inconel 718, and Greek Ascoloy) typically used for compressor blade materials. This coating was evaluated with larger (No. 90) grits in the METCO 443 matrix and lower (10 and 25 percent) grit concentration levels than evaluated in Phase 1.

The results of microscopic examinations as well as rub and erosion tests were evaluated to assess the effect that these material variations had on the coating performance. A summary of this Phase 2 evaluation is as follows:

Microscopic Examinations

1. Coatings with the larger No. 90 grits have increased porosity relative to coatings with small No. 150 grits, and coating porosity increases as grit concentration increases.

2. The level of oxides present at the coating-to-substrate interface was significantly less on INCO 718 and Greek Ascoloy substrates than for coatings on the Ti-6Al-4V substrates.

Erosion Testing

1. The titanium, nickel, or iron alloy substrates to which the coatings were applied had no significant effect on the coating erosion resistance.

2. The erosion resistance of the large grit coatings is very similar to that of the small grit coatings evaluated in Phase 1.

Rub Testing

1. The larger No. 90 grits did not improve the coating rub effectiveness (Volume wear ratio) when compared to the smaller No. 150 grit coatings, evaluated in Phase 1.

2. There is no clear dependency of rub effectiveness on grit concentration level. It is suspected that this is due to uncontrollable porosity, inherent to large grits, that occurs during the spray process resulting in reduced grit retention by the matrix material and weaker coating structure.

3.4.3 Phase 3 - High Temperature Coatings

This phase of the program evaluated abrasive coatings consisting of a high temperature capability TIPALOY matrix material in combination with silicon nitride and silicon carbide abrasive grits in two grit size ranges, No. 150 and No. 54. The coatings were evaluated on Inconel 718 test specimens at low and high grit concentration levels, 15-25 and 30-40 percent for small grits and 10-15 and 20-25 percent for large grits. To provide a basis for comparison, duplicate evaluations were conducted on coatings comprised of METCO 443 matrices in combination with silicon carbide and silicon nitride grits.

The results of the evaluation of these Phase 3 abrasive coating systems is described below:

Microscopic Examinations

1. The silicon nitride grits exhibited rounded features which would inhibit cutting action of the abradable and had a porous structure.

2. Coatings with large No. 54 grits exhibited large levels of porosity and poor grit retention in the matrix. Due to the sparse and poor distribution of grits along the specimen surface, the grit concentration could not be defined except by visual judgement.

Adherence Testing

1. The adhesive strengths of TIPALOY and METCO 443 matrix coatings with small abrasive grits are very similar and are well above the minimum requirements (3448 N/cm^2) generally acceptable for plasma sprayed coatings.

2. Coatings with large No. 54 grits exhibit a significant variation and reduction in bond strength relative to coatings with small grits. This variation in strength is likely due to the large levels and variations in coating porosity inherent to the plasma-spraying of large grits.

Erosion Testing

1. The erosion level of the abrasive coatings with TIPALOY matrices is generally very similar to that of coatings with METCO 443 matrices.

2. Coating grit material (silicon carbide or silicon nitride), grit size, or grit concentration did not have a significant effect on erosion.

Rub Testing

1. The rub performance, volume-wear-ratio, of coatings with silicon nitride grits is significantly lower than coatings with silicon carbide grits; this poor performance can be attributed to the poor quality of the silicon nitride grits.

2. Based on the limited amount of rub data, it is expected that TIPALOY would be a good candidate matrix material for high temperature abrasive coatings applications.

SECTION 4.0

CONCLUSIONS AND RECOMMENDATIONS

This program was conducted to evaluate various combinations of matrix and grit abrasive materials, applied using a plasma "co-spray" process, for use as an abrasive tip treatment on compressor blades. The test evaluations and microscopic examinations conducted on these materials provided the bases for the following conclusions and recommendations:

1. Plasma-sprayed abrasive coatings on compressor blade tips can improve rub performance [volume wear ratio (VWR)] by a factor of 100 and reduce blade wear by 85 to 90 percent.

2. Both METCO 443 and METCO 43C matrix materials in combination with No. 150 (0.002 to 0.005 inch) size silicon carbide grits, plasma-sprayed at 15 to 20 percent grit concentration levels performed equally well as an abrasive coating. METCO 443 was selected as the better matrix since it is a single layer system, not requiring a bond coat, that can be applied at reduced cost.

3. Abrasive grits larger than No. 150 grit size are difficult to spray on thin blade tip cross-sections, are prone to have coating porosity problems, and do not improve rub performance.

4. Coating porosity increases as grit concentration and grit size increase and is difficult to control for coatings with grit concentration levels above 30 percent and grit sizes larger than No. 150.

5. Additional development work is recommended to improve the repeatability and resolve the porosity problems associated with the "co-spray" process. The use of smaller grits in the 0.025 to 0.050 mm (0.001 to 0.002 inch) size range and/or precoated grits should substantially resolve these problems as well as improve the coating rub performance.

6. Although the TIPALOY matrix material did not exhibit as good rub performance as did METCO 443, it is judged to be a good matrix candidate for further development as an abrasive blade tip treatment for advanced engine, high temperature application.

7. Silicon nitride grit material is not recommended for use as an abrasive for producing abrasive coatings; they lose their sharp features during the spray process and produce coatings with poor rub performance.

Page Intentionally Left Blank

Director
Propulsion Laboratory M/S 302-2
U.S. Army Research & Technology
Laboratories (AVSCOM)
21000 Brookpark Road
Cleveland, OH 44135 2 Copies

Director
Applied Technology Laboratory
U.S. Army Research & Technology
Laboratories (AVSCOM)
Attn: DAVDL-ATL-AT
Ft. Eustis, VA 23604 2 Copies

Director
U.S. Army Research & Technology
Laboratories (AVSCOM)
Attn: DAVDL-AS M/S 207-5 H. Wilsted
Ames Research Center
Moffett Field, Ca 94035

Director
U.S. Army Research & Technology
Laboratories (AVSCOM)
Attn: DAVDL-POM M/S 206-4
Ames Research Center
Moffett Field, CA 94035

Commander
U.S. Army Aviation Systems Command
Attn: DRDAV-N (Titus)
4300 Goodfellow Blvd.
St. Louis, MO 63120

Commander
U.S. Army Aviation Systems Command
Attn: DRDAV-EQP
4300 Goodfellow Blvd.
St. Louis, MO 63120

Commander
U.S. Army Troop Support Command
Attn: DRSTS-DIL
4300 Goodfellow Blvd.
St. Louis, MO 63120 12 Copies

Commander
U.S. Army Mobility Equipment R & D
Command
Attn: DRDME-ZT, Mr. Dinger
Ft. Belvoir, VA 22060

Commander
U.S. Army Tank-Automotive R & D
Command
Attn: DRDTA-RGE, Mr. Whitcomb
Warren, MI 48090

Dr. Donald Dix
Staff Specialist for Propulsion
OSD/OUSDR&E (ET)
Rm. 1809, The Pentagon
Washington, DC 20301

Commander
Army Research Office
Attn: Dr. R. Singleton
P.O. Box 12211
Research Triangle Park, NC 27709

Commandant
U.S. Military Academy
Attn:Chief, Department of Mechanics
West Point, NY 10996

Commander
Southwest Research Institute
U.S. Army Fuels & Lubricants
Research Laboratory
P.O. Drawer 28510
San Antonio, TX 78284

Department of the Army
Aviation Systems L Division
ODCSRDA (DAMA-WSA, R. Ballard)
Room B454, The Pentagon
Washington, DC 20310

U.S. Army Material Systems Analysis
Activity
Attn: DRXSY-MP (Mr. Herbert Cohen)
Aberdeen Proving Ground, MD 21005

Director, Turbopropulsion Laboratory
Code 67Sf
Naval Postgraduate School
Monterey, CA 93940

Mr. Richard Alpaugh
U.S. DOE
1000 Independence Avenue
Washington, DC 20585

Mr. Bill Cleary
Associate Division Director
ORI, Inc.
1400 Spring Street
Silver Spring, MD 20910

John Ainsworth
Chromalloy PMT
13434 Floyd Circle
Dallas, TX 75243

Michael S. Beaton
Brunswick Corporation
Technetics Division
2000 Brunswick Lane
DeLand, FL 32724

Milton A. Beheim
NASA Lewis Research Center
Mail Stop 3-5
21000 Brookpark Road
Cleveland, OH 44135

Robert C. Bill
NASA Lewis Research Center
Mail Stop 49-6
21000 Brookpark Road
Cleveland, OH 44135

Jack Braun
University of Akron
Akron, OH 44325

John Blakey
Engine Technology Branch
AVSCOM
4300 Goodfellow Blvd.
St. Louis, MO 63120

W. R. Britsch
NASA Lewis Research Center
Mail Stop 301-2
21000 Brookpark Road
Cleveland, OH 44135

James D. Cawley
NASA Lewis Research Center
Mail Stop 23-2
21000 Brookpark Road
Cleveland, OH 44135

Fred Choy
University of Akron
Akron, OH 44325

Benjamin T. F. Chung
Dept. of Mechanical Engineering
University of Akron
Akron, OH 44325

Jerome P. Clifford
U.S. Army Applied Technology Lab.
DAVDL-ATL-ATP
Fort Eustis, VA 23604

David L. CLingman
Allison Gas Turbine Operations
P.O. Box 420, Speed Code W-5
Indianapolis, IN 46206

Clark V. Cooper
United Technologies Research Center
Silver Lane
East Hartford, CT 06108

David Day
Brunswick Corporation
Technetics Division
2000 Brunswick Lane
DeLand, FL 32724

Robert P. Dengler
NASA Lewis Research Center
Mail Stop 301-4
21000 Brookpark Road
Cleveland, OH 44135

Dan Dougherty
General Tire Corp.
Akron, OH 44325

C. Elrod
AFWAL/POTX
Wright-Patterson AFB, OH 45433

Robert L. Fusaro
NASA Lewis Research Center
Mail Stop 23-2
Cleveland, OH 44135

Roy D. Hager
NASA Lewis Research Center
Mail Stop 301-4
21000 Brookpark Road
Cleveland, OH 44135

Nabil S. Hakim
Detroit Diesel Allison
Speed Code R03B
36880 Ecorse Road
Romulus, MI 48174

John W. Halloran
C.W.R.U
10900 Euclid Avenue
Cleveland, OH 44106

Robert F. Handschuh
NASA Lewis Research Center
Mail Stop 23-2
21000 Brookpark Road
Cleveland, OH 44135 30 Copies

Robert C. Hendricks
NASA Lewis Research Center
Mail Stop 23-2
21000 Brookpark Road
Cleveland, OH 44135

Albert F. Kascak
NASA Lewis Research Center
Mail Stop 23-2
21000 Brookpark Road
Cleveland, OH 44135

E. J. Kawecki
M.S. 713-15
Pratt & Whitney Aircraft
P.O. Box 2691
West Palm Beach, FL 33458

Francis E. Kennedy, Jr.
Dartmouth College
Thayer School of Engineering
Hanover, NH 03755

L. James Kiraly
NASA Lewis Research Center
Mail Stop 23-2
21000 Brookpark Road
Cleveland, OH 44135

George Kovacich
Chief, Engine Technology Branch
AVSCOM
4300 Goodfellow Blvd.
St. Louis, MO 63120

R. Martin
AFWAL
Wright-Patterson AFB, OH 45433

Glen E. McDonald
NASA Lewis Research Center
Mail Stop 23-3
21000 Brookpark Road
Cleveland, OH 44135

James J. McLaughlin
Teledyne CAE
1330 Laskey Road
Toledo, OH 43612

Daniel B. Miracle
AFWAL/MLLM
Wright-Patterson AFB, OH 45433

Robert L. Mullen
Dept. of Civil Engineering
C.W.R.U.
Cleveland, OH 44106

Stephen T. Narsavage
Pratt & Whitney Aircraft
P.O. Box 2691
West Palm Beach, FL 33402

Joe Padovan
University of Akron
Akron, OH 44325

Robert J. Petruska
Naval Air Propulsion Center
P.O. Box 7176
Trenton, NJ 08628

P. V. Rao
NASA Lewis Research Center
Mail Stop 23-2
21000 Brookpark Road
Cleveland, OH 44135

Harry Saddock
Chromalloy PMT
13434 Floyd Circle
Dallas, TX 75243

Jerry D. Schell
General Electric
Mail Drop H99
1 Nuemann Way
Evendale, OH 45215

Robert C. Schwab
General Electric Co.
Mail Drop M87
1 Neumann Way
Evendale, OH 45215

R. Shepler
Chromalloy PMT
13434 Floyd Circle
Dallas, TX 75243

Harold L. Stocker
Allison Gas Turbines
P.O. Box 420
Indianapolis, IN 46206

Thomas N. Strom
NASA Lewis Research Center
Mail Stop 23-2
21000 Brookpark Road
Cleveland, OH 44135

Thomas A. Taylor
Materials Development Manager
Union Carbide Corp.,
Coatings Service
1500 Polco Street
Indianapolis, IN 46224

Robert P. Tolokan
Brunswick Corporation
Technetics Division
2000 Brunswick Lane
DeLand, FL 32724

Keith Topham
AFWAL
Wright-Patterson AFB, OH 45433

Y. I. Wassef
NASA Lewis Research Center
Mail Stop 500-212
21000 Brookpark Road
Cleveland, OH 44135

J. Wolak
University of Washington
Dept. of Mechanical Engineering
FU-10
Seattle, WA 98195

J. A. Ziemianski
NASA Lewis Research Center
Mail Stop 49-6
21000 Brookpark Road
Cleveland, OH 44135

D. J. Gauntner
NASA Lewis Research Center
Mail Stop 23-2
21000 Brookpark Road
Cleveland, OH 44135

NASA Scientific and Tech Inf Facility
P.O. Box 8757
B.W.I. Airport, Maryland 21240